

# Rift-related magmatism of the Central Atlantic magmatic province in Algarve, Southern Portugal

L.T. Martins <sup>a,\*</sup>, J. Madeira <sup>b</sup>, N. Youbi <sup>c</sup>, J. Munhá <sup>a</sup>, J. Mata <sup>a</sup>, R. Kerrich <sup>d</sup>

<sup>a</sup> Departamento de Geologia da Faculdade de Ciências, Universidade de Lisboa, CeGUL, Edif. C6, Campo Grande, 1749-016 Lisboa, Portugal

<sup>b</sup> Departamento de Geologia da Faculdade de Ciências, Universidade de Lisboa, LATTEX and IDL, Edif. C6, Campo Grande, 1749-016 Lisboa, Portugal

<sup>c</sup> Department of Geology, Faculty of Sciences-Semlalia, Cadi Ayyad University, P.O. Box. 2390, Prince Moulay Abdellah Avenue, Marrakech 40000, Morocco

<sup>d</sup> Department of Geological Sciences, University of Saskatchewan, Saskatoon, Canada S7N 5E2

Received 2 March 2006; accepted 10 July 2007

Available online 7 August 2007

## Abstract

Lower Jurassic volcanic-sedimentary successions of the Algarve Basin (~198 Ma) are associated with the Central Atlantic Magmatic Province (CAMP), that was one aspect of Pangean intracontinental rifting. Volcanic products of the Algarve CAMP include subaerial lava flows, pyroclastic deposits and peperites, and contemporaneous sedimentation is dominated by mudstones and conglomerates, often containing volcanic fragments, intercalated in the volcanic sequence. These lithological characteristics and associations are compatible with a facies model typical of continental basaltic magmatism. Volcanic rocks are fractionated low-Ti tholeiites enriched in large ion lithophile elements relative to high field strength elements. The compositional spectrum (e.g., Ba/Nb–Zr/Nb) is consistent with derivation of primary magmas by partial melting of heterogeneous sources, initially continental lithospheric mantle progressively replaced by an asthenospheric source. Fractional crystallization processes occurred in magma chambers located at depths close to the crust/mantle boundary from density and geobarometric constraints, reflecting magma underplating during the initial stages of continental rifting. Sporadic occurrence of crustal xenoliths, widespread evidence for basement carbonate assimilation, as well as Sr ( $(^{87}\text{Sr}/^{86}\text{Sr})_0 > 0.7050$ ) and oxygen ( $\delta^{18}\text{O} > +7.40\%$ ) isotope ratios that are higher than those typical of continental lithospheric mantle, indicate that crustal contamination also contributed to the observed geochemical variations. The Carnian–Norian (228.0 to 203.6 Ma) or older age estimated for the basal Silves Sandstones suggests that the inception of rift related sedimentation preceded volcanism by 20 to 30 Ma. These results lead us to propose a passive rifting model for the Algarve sector of CAMP magmatism, the orientation of which was conditioned by strain localization along pre-existing lithospheric mechanical anisotropies.

© 2007 Published by Elsevier B.V.

**Keywords:** CAMP magmatism; Portugal; Pangean continental rifting; Volcanostratigraphy; Low-Ti tholeiites; Assimilation-fractional crystallization

\* Corresponding author. Tel.: +351 217500066; fax: +351 217500064.

E-mail addresses: [lmartins@fc.ul.pt](mailto:lmartins@fc.ul.pt) (L.T. Martins), [jmadeira@fc.ul.pt](mailto:jmadeira@fc.ul.pt) (J. Madeira), [youbi@ucam.ac.ma](mailto:youbi@ucam.ac.ma) (N. Youbi), [jmunha@fc.ul.pt](mailto:jmunha@fc.ul.pt) (J. Munhá), [jmata@fc.ul.pt](mailto:jmata@fc.ul.pt) (J. Mata), [robert.kerrich@usask.ca](mailto:robert.kerrich@usask.ca) (R. Kerrich).

## 1. Introduction

Magmatism is generally active at different stages of continental fragmentation. From the inception of continental rifting to the final oceanic stage, magmatism

represents evolution from a continental intra-plate geodynamic setting to a passive continental margin, the latter also termed a volcanic passive margin. The variety of magmas inform us about the sources of the magmas and, therefore, about the dynamics of the mantle, in particular on asthenosphere–lithosphere interactions (Lassiter and DePaolo, 1997; Head and Coffin, 1997).

Pangean intracontinental rifting, that led to the future Central Atlantic ocean, commenced in the Upper Permian–Lower Triassic (Ruellan, 1985; Ruellan et al., 1985; Medina, 1995; 2000; El Arabi et al., 2006), progressing from South towards North following the direction of the late Paleozoic Alleghenian–Hercynian orogenic chain. Mapping and dating of the magnetic anomaly couples made it possible to constrain 170–175 Ma (Middle Jurassic) as the beginning of oceanic opening (Klitgord and Schouten, 1986). Similar ages (178–180 Ma) were obtained from xenoliths of metagabbros and metabasalts, occurring in association with Neogene to Recent volcanism on Canary Island; given mid ocean ridge basalt (MORB) trace element signatures, the xenoliths were interpreted as fragments of subjacent Mesozoic oceanic crust (Schmincke et al., 1998; Hoernle, 1998). Recent reconstructions of the opening of the Central Atlantic Ocean (Sahabi et al., 2004), which take into account the African equivalent of the East Coast Magnetic Anomaly as well as the extension of the Triassic–Jurassic evaporite basins from Morocco and Nova Scotia, place the age of the earliest oceanic crust in the Central Atlantic at the end of the Sinemurian (196.5 to 189.6 Ma). This is 20 Ma earlier than the age proposed by Klitgord and Schouten (1986).

Pangean rifting was accompanied by a Large Igneous Province (LIP), known as the Central Atlantic Magmatic Province (CAMP; Marzoli et al., 1999), mainly composed of low-Ti tholeiitic Continental Flood Basalts (CFB). CAMP magmatism is nowadays represented by remnants of intrusive (crustal underplates, layered intrusions, sills, dikes) and extrusive (pyroclastic sequences and lava flows) rocks that occur in once-contiguous parts of North and South America, northwestern Africa, and southwestern Europe (Marzoli et al., 1999; McHone and Puffer, 2003). This LIP may have extended over  $7 \times 10^6$  km<sup>2</sup>, with a total volume of magma estimated at  $2\text{--}4 \times 10^6$  km<sup>3</sup> (Marzoli et al., 1999; Olsen, 1999). The Central Atlantic LIP is considered the result of a mantle super-plume (e.g. Oyarzun et al., 1997; Wilson, 1997) or, alternatively, as a consequence of lithosphere extension and thinning, pre-dating the Atlantic opening, that triggered decompressional melting in the upper asthenosphere (Withjack et al., 1998; Medina, 2000). Magmatism is apparently coeval with the mass extinction at the Triassic–Jurassic boundary (e.g. Nomade et al., 2007).

In this paper we present new volcanostratigraphic and geochemical data for CAMP related magmatism from the Algarve, Southern Portugal, in order to: (1) characterize the Algarve magmatic activity and coeval sedimentation, and thus develop a facies model; (2) constrain sources of basaltic lavas, either in the continental lithospheric mantle, asthenosphere, or some combination; (3) address possible crustal contamination; (4) contribute to the understanding of the type of rifting mechanism, whether active or passive; and (5) better characterize the lower Mesozoic Central Atlantic Magmatism.

## 2. Geologic setting

Early Jurassic volcanic rocks of Portugal constitute an interesting sub-province of the CAMP as most of the exposed outcrops are extrusive. Volcanic units are preserved in graben and semi-graben structures trending NNE–SSW in the Santiago do Cacém Basin, and E–W in the Algarve Basin (Fig. 1). The Lower Mesozoic of the Algarve Basin rests unconformably on Variscan basement, which comprises Visean (345.3 to 326.4 Ma) limestone and marl formations overlain by flysch of Namurian to Westphalian age (326.4 to 306.4 Ma; Gradstein et al., 2004; Manuppella, 1992).

Lower Mesozoic sedimentation commenced with continental clastic deposits (conglomerates, red sandstones and pelites), followed by deposition of continental and littoral red pelites, locally containing thin layers of limestone or dolomite, and evaporites. Together, these form the unit of the Silves Sandstones s.l. (Palain, 1979). Carbonates of Sinemurian age (196.5 to 189.6 Ma) were deposited as the basin became gradually deeper and the region was progressively invaded by the sea (Rocha, 1976; Palain, 1979; Rey, 1983; Manuppella, 1988, 1992).

The CAMP volcanic sequence is interlayered within the red pelites, termed the Pelite–Carbonate–Evaporite Complex by Manuppella (1992). The volcanic rocks overlie a 100 to 375 m thick sedimentary sequence composed of pelites and conglomerates (unit AA of Palain, 1979), sandstones (unit AB1), pelites (unit AB2) and thin carbonate layers interbedded in pelites (unit AB3).

Rare paleontological remains have been documented in the Silves Sandstones. These include: bones of *Stegoccephalus* in the pelites of the AA unit; *Euestheria minuta* and *Pseudoasmussia destombesi* in the upper part of AB1; palinological associations of Triassic affinity in the lower part of AB2; and Hettangian lamellibranches and gastropods in the dolomites of AB3 (Palain, 1979; Manuppella, 1988, 1992, and references therein). These associations are consistent with an Upper Triassic age (228 to 199.6 Ma) for units AA, AB1 and lower part of

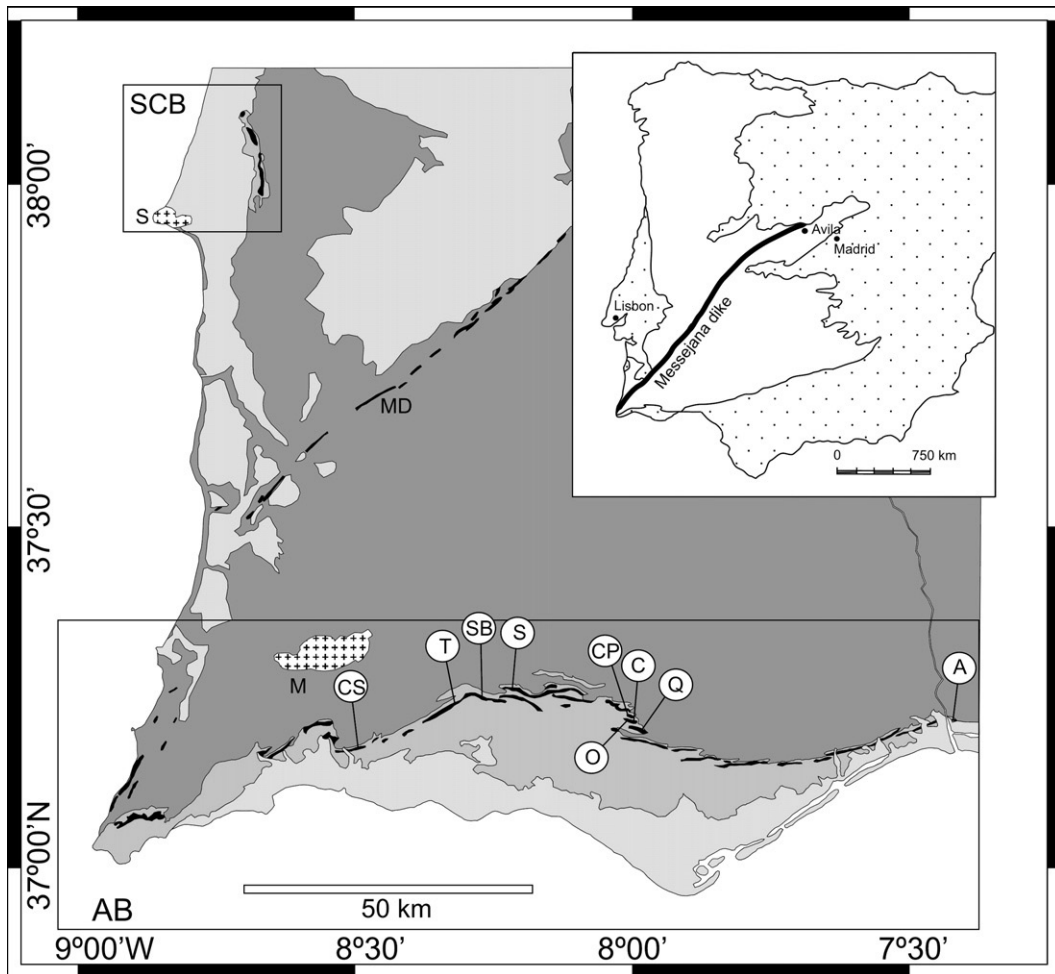


Fig. 1. Geographical and geological setting of the CAMP rocks in Iberia: location of Mesesjana Dike (inset), Santiago do Cacém (SCB) and Algarve (AB) Basins. Dark grey — pre Mesozoic rocks; medium grey — Mesozoic rocks; light grey — post Mesozoic cover; crosses — Late Cretaceous sub-volcanic complexes of Sines (S) and Monchique (M); black — CAMP extrusive sequences and Mesesjana Dike (MD). Circles indicate localities referred in text or depicted in logs or geologic sections: CS — Cabeças-Silves; T — Torre; SB — S. Bartolomeu de Messines; S — Soidos; CP — Cerro dos Passarinhos; O — Quinta da Ombria; C — Corcitos; Q — Querença; A — Ayamonte (Appendix A).

AB2, but a Hettangian age (199.6 to 196.5 Ma) for the uppermost part of AB2 and unit AB3. In the Lusitanian Basin, the base of unit A2 (correlative with unit AB2 from the Algarve Basin) yielded an association of pollens and spores of Carnian–Norian age (228.0 to 203.6 Ma), indicating an older age for the base of those sediments (Palain, 1979).

### 3. Physical volcanology and facies model for the portuguese CAMP

#### 3.1. Background context

CAMP volcanic sequences from the Algarve Basin have never been studied from the volcanological and

stratigraphic point of view. Former studies deal with the general stratigraphy of the base of the Mesozoic in Algarve (Palain, 1979), regional scale geological mapping (Manuppella, 1988; 1992), petrology and geochemistry (e.g. Martins, 1991; Martins and Kerrich, 1998; Youbi et al., 2003), and geochronology (Verati et al., 2007).

We present the results of recent fieldwork focused on characterizing the volcanic sequence in the most representative and complete outcrops of the Algarve basin (Fig. 1). This work documents several stratigraphic sections, leads to an interpretation for the environment in which the volcanism occurred, and supplies a stratigraphic framework for petrological and geochemical analyses.

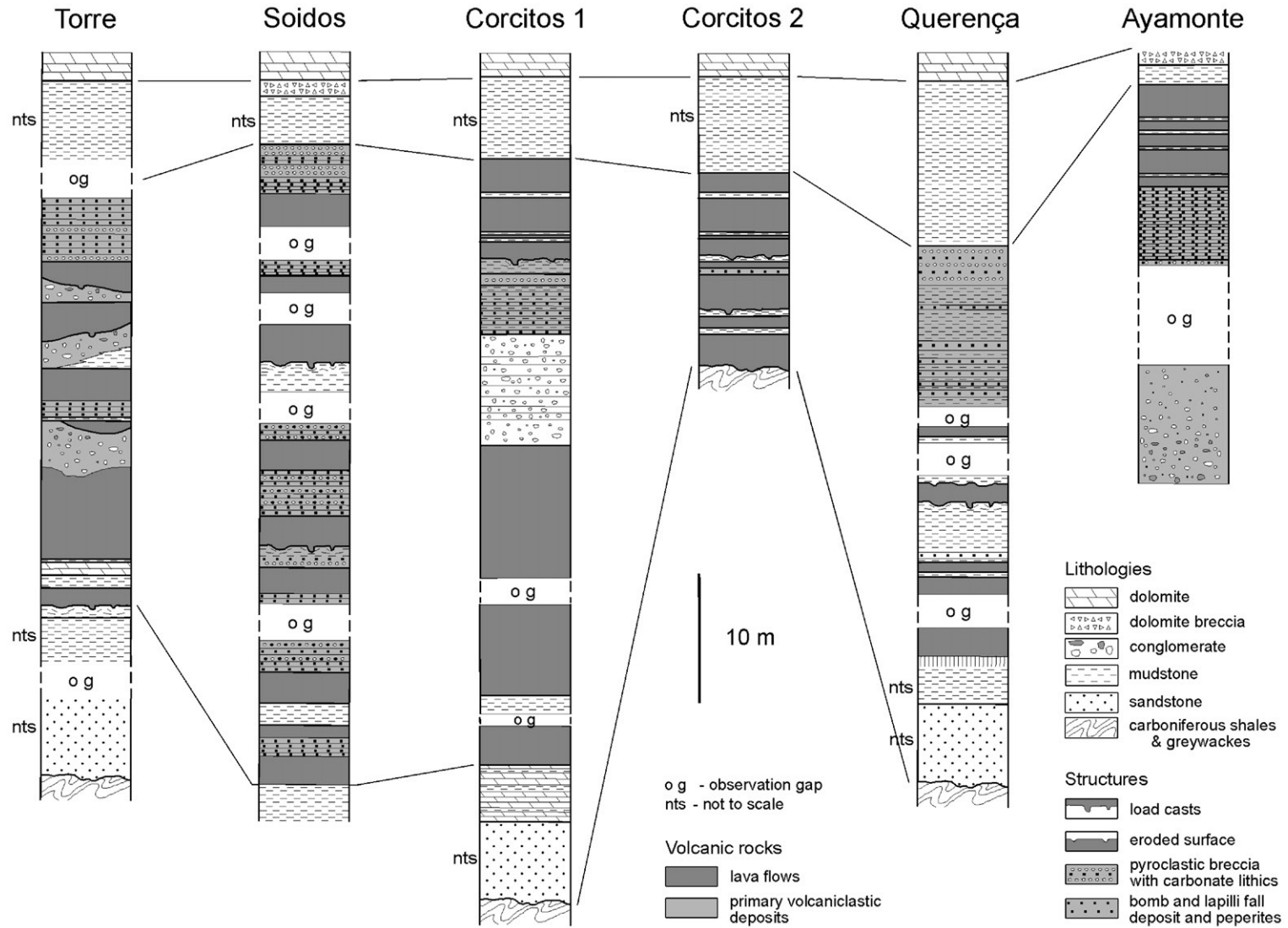


Fig. 2. Stratigraphic logs of the most continuous and complete geological sections (see Fig. 1 and Appendix A for geographic locations).

The best outcrops are located in central Algarve, where the sequences are thicker. To the west the volcano-sedimentary pile becomes thinner and the quality of outcrop deteriorates. An excellent section was recently exposed in the new road linking the Portugal-Spain highway to the village of Ayamonte (Spain), corresponding to the easternmost outcrop of the Algarve Basin CAMP sequence. In this study the descriptions were based mainly in the Cabeças–Silves, Torre, S. Bartolomeu de Messines, Soidos, Querença, Corcitos, and Ayamonte sections, which are graphically presented as stratigraphic logs in Fig. 2 (locations given in Appendix A).

The total thickness of the preserved volcano-sedimentary pile varies between 30 and 50m. Five to eight lava flows are present in the most complete sections. In many sections it is not possible to be certain of the number of lava flows due to observational gaps; for instance, lava outcrops separated by observational gaps may belong to the same or to different flows. The number of eruptive events represented by the preserved/observed deposits in

any single section is uncertain. Unlike the Moroccan CAMP volcanism where four units have been established (Youbi et al., 2003 and references therein), the sequences in Algarve are so variable from section to section that it is not possible to establish a characteristic type section. Most CAMP volcanism in the Algarve Basin is composed of extrusive sequences. Sequences present alternating deposits of effusive and explosive events that are not correlatable from section to section, even if geographically close. Lava flows and primary volcaniclastic deposits (White and Houghton, 2006) are equally abundant: lava flows, peperites and pyroclastic deposits are generally associated in the most complete sequences. Sediments are typically inter-bedded with extrusive units. Feeder structures such as dikes, pipes and sills are rare, and eruptive centres have never been recognised.

Lithological characteristics and thickness of sediments must be related to the contemporaneous morphology and dimensions of the basins, and to syn-volcanic/sedimentary tectonics. The different types of igneous occurrences in the CAMP of the Algarve Basin

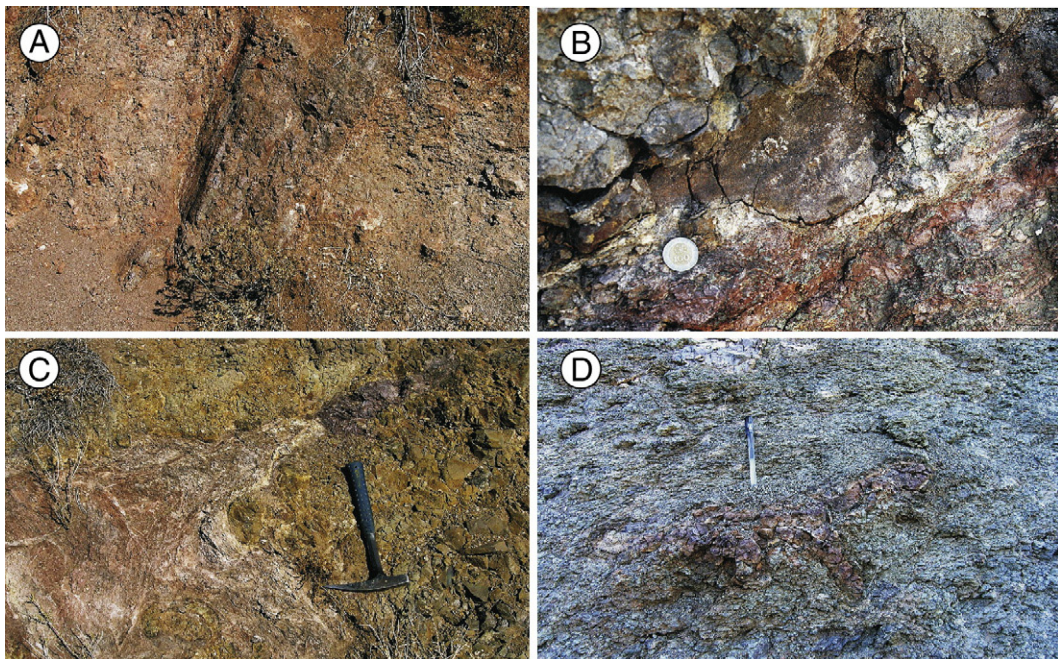


Fig. 3. Some field characteristics of CAMP sequences in Algarve: A — 1 m wide dike cutting through phreato-magmatic deposits in the middle part of the Querença section; B — small load cast of lava flow base into pyroclastic-rich clayey sediment (Corcitos section); C — highly convoluted base of the fifth lava flow of the Soidos section sinking into and deforming red mudstone; D — peperite with a large fluidal shaped lava fragment in a finer volcaniclastic matrix (Querença section); E — detail of the contact of a lava flow base with red mudstone marked by 1 to 2 cm of chilled glass (Corcitos); F — sequence of alternating pyroclast (pale green) and clay/silt (dark red) layers (Quinta da Ombria); G — vertical pipe vesicles rising 30 to 50 cm from base of lava flow (S. Bartolomeu de Messines); H — alternating light grey mudstone layers (pale colour) and greenish/brown pyroclastic deposit (darker) in the middle part of the Ayamonte section; note the normal faults affecting the sequence (encircled pen gives scale); I — injection of red clay upwards into vertical fracture in lava flow; the block to the left has sunk 1.5 m and the fracture does not extend to the underlying lava flow (S. Bartolomeu de Messines); J — light grey clay matrix conglomerate containing big blocks of basalt and carbonate, from the base of the Ayamonte section.

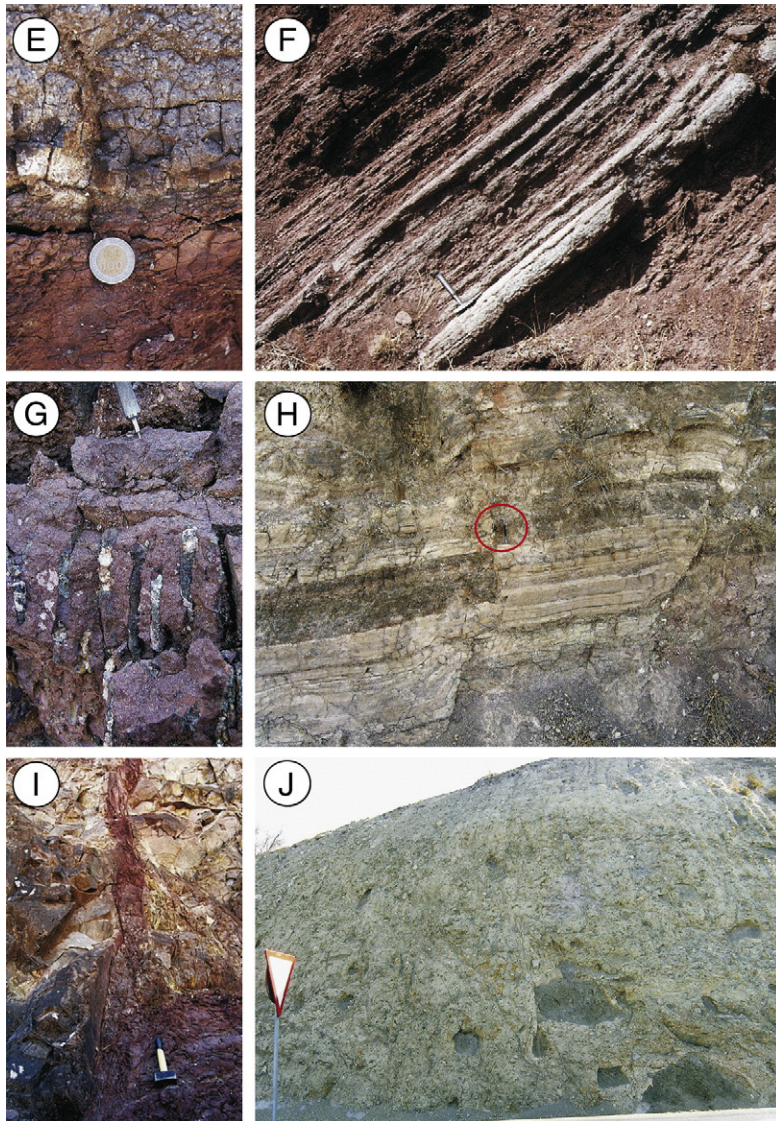


Fig. 3 (continued).

and their characteristics are described below. All interpretations are constrained by limitations of outcrop and weathering.

### 3.2. Feeder structures

The NE-SW Messejana dike constitutes an important geological feature, and may represent the major feeder structure for CAMP volcanism in Iberia (Schermerhorn et al., 1978; Schott et al., 1981; Alibert, 1984; Sebai et al., 1991; Dunn et al., 1998; Cebriá et al., 2003; Palencia Ortas et al., 2006). The dike extends NE for up to 530 km from the SW coast of Portugal to the centre of Iberia, and the thickness varies from 5m up to 300m,

including splays (Fig. 1) This intrusion transects Hercynian structures in Precambrian and Palaeozoic terranes, and is locally covered by Cenozoic formations. However, there is no present field relationship between the Messejana dike and outcrops of extrusive sequences of the same age, which are physiographically isolated from that structure. Erosion has removed the upper part of the dike, the contemporaneous topographic surface and presumed extrusive products. Accordingly, it is inconclusive as to whether or not the Messejana dike fed the volcanic sequences in the Algarve.

Varied other intrusions have been observed. These include: sporadic, thin (less than 1m wide) dikes cutting the extrusive volcanic sequences (Fig. 3-A); some

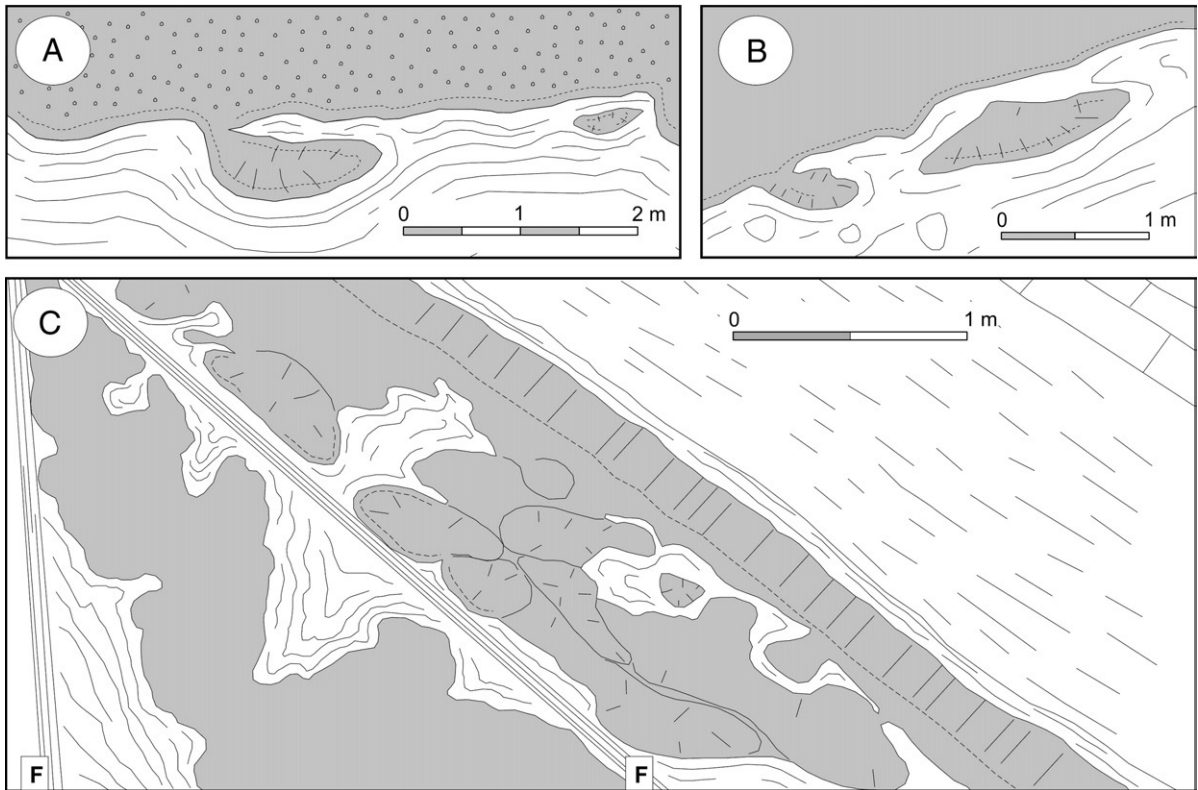


Fig. 4. Field sketches of bases of lavas that flowed over soft sediments (lava in grey, sediments in white): A — base of vesicular flow penetrating red clay sediment; the sunken portions show incipient radial joints (Corcitos); B — identical situation in a lava flow from the Torre section, flowing over red clay matrix conglomerate; C — irregular geometry of the lower flow from the Torre section as a result of mingling with soft sediment. Flow is divided in two by faulting (F); the lower portion is an irregular body of lava totally immersed in deformed light-grey-silty-clay; the base of the upper portion is partly sunken into the sediment forming pillow-like structures (or lava toes), but has a regular (formerly horizontal) surface, with 20–30 cm long vertical pipe vesicles. Light-grey clay and marly sediments cover the flow.

tabular magmatic bodies that may correspond to shallow sills intruded into the volcano-sedimentary deposits; and a few possible pipes represented by massive magmatic rock outcrops without lateral continuity. A few dikes were observed intruding the complete thickness of the lava flows and pyroclastic deposits, indicative that the volcanic sequence is not completely preserved in the geological record. The upper part of the extrusive sequence (of unknown thickness), including probable

local eruptive centres fed by those intrusions (e.g. lapilli and scoria cones, scoria ramparts, tuff rings, tuff cones, and maars), has been removed by contemporaneous and subsequent early Jurassic erosion.

### 3.3. Volcanic rocks

Volcanic CAMP units include extrusive and secondary volcanoclastic deposits. The former are represented

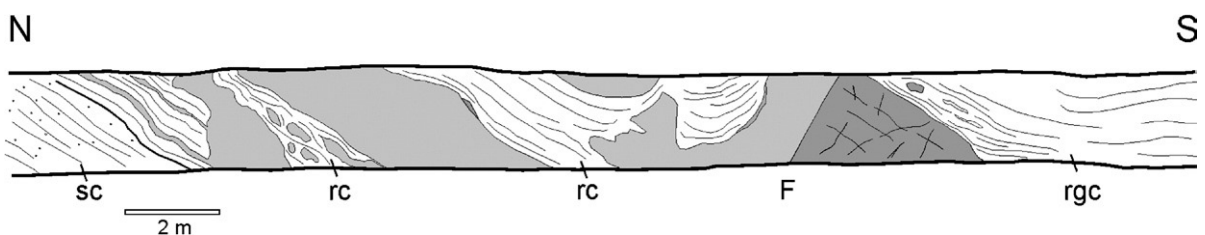


Fig. 5. Field sketch of the Cabeças-Silves section: shallow intrusions of two magma bodies (light and dark grey) into a soft unconsolidated sedimentary sequence forming irregular sills. sc — green sandy clay; rc — red clay; rgc — red and grey clays; F — fault.

Table 1  
Representative olivine and clinopyroxene chemistry of Lower Jurassic rocks from the Algarve CAMP (Martins, 1991)

Sample	Olivines <sup>a</sup>		Olivines <sup>b</sup>		Sample	Clinopyroxenes <sup>a</sup>				Clinopyroxenes <sup>b</sup>						
	R2-13		R2-4	E5-1		R2-13		E4-2	E1-2	E7-2	E5-1		R2-31		E2-4	
	1	2	1*	2		1	2	3	4	Core	Rim	Core	Rim	Core	Rim	
SiO <sub>2</sub> (wt.%)	35.21	34.37	35.97	34.78	SiO <sub>2</sub> (wt.%)	51.15	53.89	53.04	54.06	53.37	52.97	54.19	47.35	52.99	47.04	
TiO <sub>2</sub>	0.00	0.00	0.00	0.00	TiO <sub>2</sub>	0.88	0.29	0.35	0.21	0.28	0.32	0.27	1.39	0.30	1.06	
Al <sub>2</sub> O <sub>3</sub>	0.02	0.03	0.04	0.00	Al <sub>2</sub> O <sub>3</sub>	1.93	1.25	0.91	0.84	1.90	2.23	1.35	6.21	2.65	9.11	
Cr <sub>2</sub> O <sub>3</sub>	0.00	0.00	0.00	0.00	Cr <sub>2</sub> O <sub>3</sub>	0.04	0.19	0.07	0.00	0.70	0.55	0.27	0.06	0.60	0.06	
NiO	0.03	0.11	0.04	0.07	Fe <sub>2</sub> O <sub>3</sub>	1.92	0.00	0.00	0.97	0.00	0.49	0.31	4.15	0.00	0.00	
FeO	41.01	43.11	33.01	42.39	FeO	9.39	8.68	20.44	15.12	5.37	5.92	5.21	6.84	5.15	9.14	
MnO	0.71	0.75	0.56	0.61	MnO	0.19	0.26	0.33	0.29	0.14	0.13	0.18	0.17	0.11	0.13	
MgO	23.16	21.79	29.83	22.07	MgO	12.54	19.36	19.94	24.75	18.09	17.44	16.50	10.19	15.40	9.16	
CaO	0.30	0.32	0.27	0.19	CaO	21.48	15.78	5.26	4.15	19.44	20.03	21.54	23.20	22.26	22.81	
Total	100.44	100.48	99.72	100.11	Na <sub>2</sub> O	0.54	0.16	0.08	0.03	0.21	0.18	0.57	0.64	0.48	0.49	
Number of ions on the basis of 4 oxygens					K <sub>2</sub> O	0.00	0.00	0.00	0.00	0.00	0.00	0.00	0.00	0.00	0.00	
Si	1.004	0.993	0.993	1.003	Total	100.06	99.86	100.42	100.42	99.50	100.26	100.39	100.20	99.94	99.00	
Al (IV)	0.000	0.001	0.001	0.000	Number of ions on the basis of 4 cations											
Al (VI)	0.001	0.000	0.000	0.000	Si	1.924	1.972	1.977	1.962	1.955	1.935	1.976	1.786	1.785	1.946	
Ti	0.000	0.000	0.000	0.000	Al (IV)	0.076	0.028	0.023	0.036	0.045	0.065	0.024	0.214	0.215	0.054	
Cr	0.000	0.000	0.000	0.000	Al (VI)	0.010	0.026	0.017	0.000	0.037	0.031	0.034	0.062	0.192	0.060	
Ni	0.001	0.003	0.001	0.002	Ti	0.025	0.008	0.010	0.006	0.008	0.009	0.007	0.039	0.030	0.008	
Fe <sup>2+</sup>	0.978	1.042	0.762	1.022	Cr	0.001	0.005	0.002	0.000	0.020	0.016	0.008	0.002	0.002	0.017	
Mn	0.017	0.018	0.013	0.015	Fe <sup>3+</sup>	0.054	0.000	0.000	0.027	0.000	0.014	0.008	0.118	0.000	0.000	
Mg	0.985	0.939	1.228	0.949	Fe <sup>2+</sup>	0.295	0.266	0.637	0.459	0.165	0.181	0.159	0.216	0.290	0.158	
Ca	0.009	0.010	0.008	0.006	Mn	0.006	0.008	0.010	0.009	0.004	0.004	0.006	0.005	0.004	0.003	
Fo %	50.18	47.40	61.71	48.15	Mg	0.703	1.056	1.108	1.339	0.988	0.950	0.897	0.573	0.518	0.843	
*Inclusion in clinopyroxene					Ca	0.866	0.619	0.210	0.161	0.763	0.784	0.841	0.938	0.927	0.876	
					Na	0.039	0.011	0.006	0.002	0.015	0.013	0.040	0.047	0.036	0.034	
					K	0.000	0.000	0.000	0.000	0.000	0.000	0.000	0.000	0.000	0.000	
					Wo (atom%)	45.01	31.76	10.68	8.07	39.74	40.56	44.01	50.70	53.30	46.60	
					En	36.54	54.18	56.39	67.12	51.46	49.15	46.94	30.97	29.79	44.84	
					Fs	18.45	14.06	32.93	24.81	8.80	10.29	9.05	18.33	16.91	8.56	

<sup>a</sup>Tholeiitic rocks, R2-13, E4-2, E1-2, E1-2 and E7-2 whole rock analysis in Table 2.

<sup>b</sup>High-CaO porphyritic rock domains, R2-4, E5-1, R2-31 and E2-4 whole rock analysis in Table 3.

Fe<sub>2</sub>O<sub>3</sub> in clinopyroxenes according to Papike et al. (1974).

by subaerial lava flows, peperites and pyroclastic deposits, and the latter by contemporaneous resedimented volcanic material (tuffites and sediments containing dense lava fragments). Sedimentary layers are interbedded with effusive and explosive volcanic products, giving combined volcano-sedimentary sequences, indicative of coeval volcanism and sedimentation.

Lava flows are of the pahoehoe type; brecciated clinkery envelopes, typical of aa flows are absent. Most lava flows have vitreous chilled bases a few centimetres thick as a result of rapid cooling in contact with the ground (Fig. 3-E). The lava has thermally metamorphosed the underlying sediments or soils. Vaporization of water from soils or sediments overlain by lavas generated frequent vertical pipe vesicles originating from the base of lava flows (Fig. 3-G). In the Ayamonte section, trains of bubbles departing from near the base of the flows created vertical inverted cones of vesicular rock; these start with a diameter of approximately 1cm near the base of the flow and may be 6cm wide where they link to the upper vesicular lava crust. This may represent exsolution of gases in the molten interior of a stagnant flow (like bubbles rising in a glass of beer).

Most commonly, lava flows are 1 to 5 m thick, but may reach some tens of metres, have massive or platy jointed bases and vesicular upper parts often with a thin glassy outer shell, and occasionally present ill-defined columnar jointing. Sporadically, as at Corcitos, the upper surface of the flow is truncated recording the occurrence of erosive episodes between emplacement of the flow and the deposition of the overlying sediments, pyroclastic deposit or flow.

Abundant volcanoclastic units are present. Interpretation of the volcanoclastic sequences is difficult, given the extreme degree of weathering of pyroclastic particles that show greenish (or brown) colour, in contrast with the prevailing red coloured mudstones.

There are layers of clast-supported coarse ash to fine lapilli tuff, sometimes containing magmatic clasts of bomb dimensions; spaces between volcanic particles are filled with fine red sediment, which may represent infiltration from overlying sediments. This type of volcanoclastic layer is usually interbedded with layers rich in volcanic fragments supported by a clay/silty matrix. Both types of deposits form well-stratified sequences (Fig. 3-F, H). Typically there are alternating successions of red and green layers, or alternatively red (sedimentary?) layers with variable density of green spots (lapilli and ash particles). Clast-supported lapilli and ash is interpreted as in situ magmatic pyroclastic fall deposits. Matrix-supported volcanoclastic rich layers can be interpreted

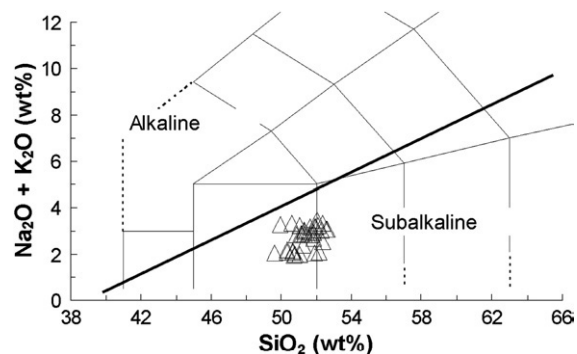


Fig. 6. The subalkaline character of the Algarve Lower Jurassic lavas is evident on a TAS diagram (Le Bas et al., 1986). The compositional divider between alkaline and subalkaline series was taken from MacDonald and Katsura (1964).

as either phreato-magmatic fall and/or flow deposits or as resedimented syn-eruptive volcanoclastic deposits (tuffites). The well-developed stratification and decimetric thickness of the layers are not compatible with the characteristic massive structure of peperite deposits, although both lithotypes involve mixtures of volcanic and sedimentary materials.

Other deposits are dominated by red silty-clay with exotic blocks. Blocks are angular limestone or dolomite fragments and mudstone balls up to 80cm in diameter, associated with juvenile lava fragments up to 40cm in diameter presenting fluidal and blocky shapes. Larger juvenile fragments are internally vesicular, present outer chilled vitreous margins and, occasionally have radial joints. This type of deposit can be interpreted as pyroclastic fallout of juvenile and lithic clasts into unconsolidated sediment, although a peperitic nature cannot be ruled out. Lithic fragments represent shattering of limestone or dolomite layers, and disruption of mudstone deposits, from the formations that underlie the volcanic sequence by phreatomagmatic processes. Notable examples are units AB2 and AB3 of *Palain* (1979, or the Pelite–Carbonate–Evaporite Complex of *Manuppella*, 1988, 1992). Hydro-magmatic characteristics include a significant fraction of irregularly shaped lithic fragments of variable dimensions and nature, and more or less developed stratification, indicating high explosivity by water-magma interaction. Both types of pyroclasts indicate a proximal location of the deposits relative to the eruptive centres, most likely scoria cones or ramparts for the magmatic events, and maars or tuff rings in the case of phreato-magmatic volcanism.

Another type of volcanoclastic deposit has the characteristics of peperites (Skilling et al., 2002, and references therein). These deposits are massive, several

Table 2

Representative major and trace element analyses of Lower Jurassic rocks from the Algarve CAMP, with a subset of Sr-and O-isotope analyses (Martins, 1991)

Sample	R2-2	R2-13	R2-37	587-6	587-7	587-8	587-9	587-14	587-15	587-16	588-3	597-5	597-9	597-21	600-1	E1-2	E4-2	E7-2
SiO <sub>2</sub> (wt.%)	50.10	49.90	50.54	51.78	52.05	50.79	51.64	50.48	50.66	49.76	50.96	51.42	50.49	51.39	51.54	51.83	51.76	49.97
TiO <sub>2</sub>	0.89	0.75	1.04	1.20	1.16	1.05	1.18	0.87	0.95	0.76	1.10	1.07	0.92	1.05	1.11	1.04	1.03	0.96
Al <sub>2</sub> O <sub>3</sub>	16.43	14.83	13.71	13.25	13.30	13.96	13.35	13.55	13.53	13.82	14.66	13.38	14.57	14.05	13.64	14.83	15.11	14.83
Fe <sub>2</sub> O <sub>3t</sub>	9.65	11.87	10.73	11.78	12.15	11.44	11.23	10.37	10.72	10.22	9.51	11.01	10.48	11.44	10.41	11.23	10.87	10.73
MnO	0.12	0.17	0.12	0.14	0.12	0.11	0.14	0.13	0.14	0.13	0.15	0.11	0.11	0.18	0.10	0.12	0.15	0.20
MgO	8.53	7.95	8.70	8.29	8.45	8.53	7.90	9.94	9.77	10.11	8.78	8.95	8.28	7.29	8.87	7.95	7.95	9.12
CaO	10.78	11.06	10.77	9.58	9.66	9.93	9.59	10.49	10.90	11.82	10.07	9.65	10.95	11.40	9.37	9.38	10.08	10.64
Na <sub>2</sub> O	1.35	2.43	2.09	2.42	2.45	2.36	2.35	2.22	2.16	1.75	2.29	2.35	2.63	2.35	2.43	1.62	1.35	1.32
K <sub>2</sub> O	0.60	0.83	0.70	0.77	0.71	0.59	0.69	0.62	0.66	0.42	0.60	0.78	0.63	0.64	0.85	0.89	0.71	0.60
P <sub>2</sub> O <sub>5</sub>	0.13	0.09	0.14	0.19	0.18	0.18	0.20	0.13	0.15	0.11	0.15	0.18	0.17	0.16	0.17	0.14	0.18	0.14
#Mg <sup>a</sup>	67.03	60.64	65.09	61.76	61.53	63.17	61.80	68.79	67.70	69.47	67.98	65.15	64.50	59.44	66.21	61.95	62.72	66.16
Sc (ppm)	32	30	36	34	35	34	35	35	39	36	35	37	34	37	35	33	34	35
V	250	266	271	302	303	293	313	261	265	250	298	284	235	259	284	228	264	270
Cr	197	225	212	63	71	129	67	237	232	-	177	98	220	197	225	151	128	203
Ni	83	65	96	56	60	62	73	101	96	116	79	76	102	74	45	64	63	84
Rb	13	8	17	26	23	16	23	13	19	14	13	-	17	19	18	19	20	14
Sr	176	639	175	177	177	168	179	183	170	153	163	157	161	167	170	179	176	164
Y	22	19	20	24	27	25	23	21	23	20	24	27	25	23	23	24	27	23
Zr	82	49	85	115	104	87	105	77	87	60	96	105	113	93	105	84	101	81
Nb	8	7	7	11	11	8	11	10	9	6	8	10	9	11	9	8	9	6
Ba	103	97	131	194	197	146	173	135	164	110	140	166	145	134	168	111	137	105.00
La				14.30				12.10	9.20		8.60			10.20				
Ce				33.00				27.00	21.00		17.00			21.00				
Nd				16.00				14.00	11.00		11.00			10.00				
Sm				3.87				3.25	2.74		2.34			3.06				
Eu				1.28				1.09	1.15		0.86			1.02				
Tb				0.80				0.60	0.60		0.50			0.60				
Yb				2.81				2.36	2.04		2.09			2.13				
Lu				0.41				0.33	0.29		0.33			0.35				
Hf				3.00				2.60	1.90		1.40			2.70				
Th				2.50				2.10	1.60		1.20			1.40				
( <sup>87</sup> Sr/ <sup>86</sup> Sr) <sub>0</sub> <sup>b</sup>				0.706205	0.706240									0.705450	0.705390			
δ <sup>18</sup> O (‰)				8.23	8.13													7.40

<sup>a</sup> Mg#=100 Mg/(Mg\*Fe<sup>2+</sup>); Fe<sup>3+</sup>/Fe<sup>2+</sup>=0.15. <sup>b</sup> Initial ratio (<sup>87</sup>Sr/<sup>86</sup>Sr)<sub>0</sub> computed at 198 Ma (based on age of Verati et al., 2007).

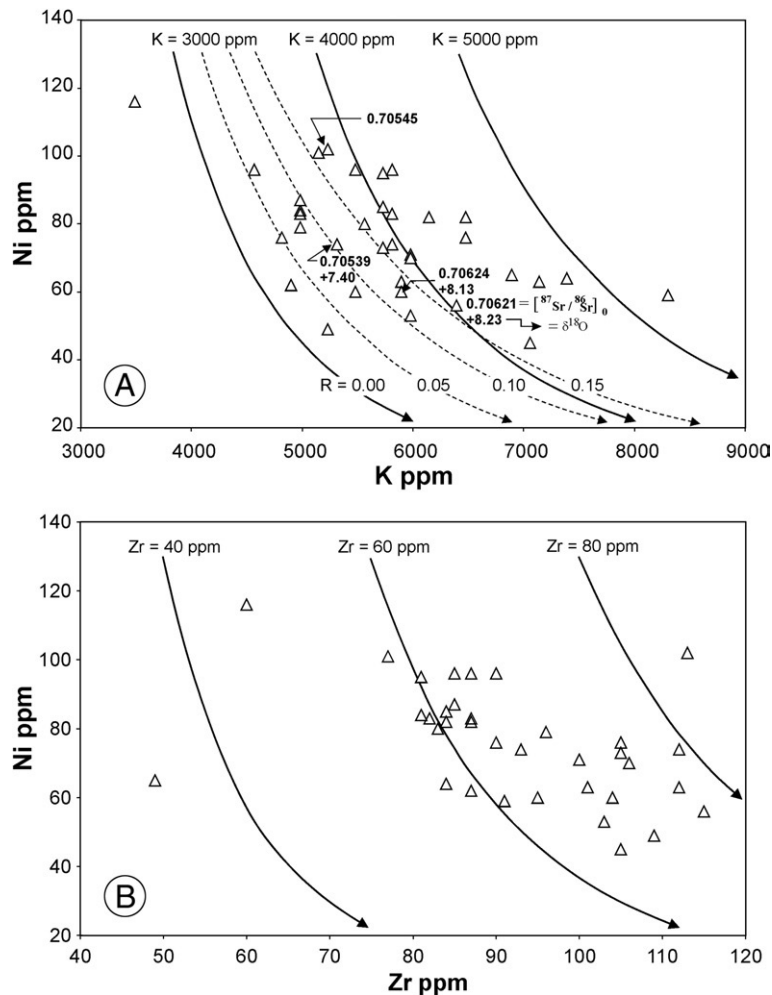


Fig. 7. (A): Ni–K relationships in tholeiitic rocks; Ni–K fractional crystallization trends for variable primary magma K contents ( $C_0^{\text{Ni}}=350$  ppm;  $D_{\text{Ni}}=5$ ;  $D_{\text{K}}=0.001$ ) and ACF (DePaolo, 1981) trends (dashed-lines) for variable relative rates of assimilation/crystallization ( $=R$ ;  $C_0^{\text{K}}(\text{magma})=3000$  ppm;  $C_{\text{Contaminant}}^{\text{K}}=23245$  ppm=average continental crust of Rudnick and Gao, 2003), as well as  $(^{87}\text{Sr}/^{86}\text{Sr})_0$  and  $\delta^{18}\text{O}$  values (see Table 2), are also shown for comparison. (B): Ni–Zr relationships in Algarve tholeiitic rocks; Ni–Zr fractional crystallization trends for variable  $C_0^{\text{Zr}}$  contents ( $D_{\text{Zr}}=0.1$ ) suggest that the Algarve tholeiitic basalts were derived from crystallization of distinct primary magmas.

metres thick, and composed of magmatic particles included in a sedimentary matrix. Most of the coarser magmatic particles are clearly juvenile, as indicated by the occurrence of fluidal shapes, glassy rinds and jointing. Fragments of ash to lapilli dimensions are irregular in shape and frequently vesicular. The sedimentary matrix is either a silty mud or a conglomerate. The density of magmatic fragments is usually high, characteristic of close-packed peperite (Fig. 3-D).

At the Cerro dos Passarinhos outcrop the peperite is associated with a coherent magma body that presents a vertical non-planar contact with the volcanoclastic deposit. This coherent domain is interpreted as the intrusion generating the peperite. Well-stratified volcanoclastic layers that cover the peperite may represent

phreatomagmatic deposits related to the same intrusion. At the Torre section, a lava flow fills a channel on a several metres thick conglomerate unit. The clasts are abundant angular limestone fragments (mm to decimetre size), and coarse juvenile brown basaltic fragments (up to 40cm) presenting fluidal, mixed and blocky morphologies and glassy rinds. The red clay matrix is rich in finer vesicular or massive green volcanoclastic fragments. This deposit may be related to initial sediment/magma interaction produced by the eruption that generated the overlying lava flow.

The stratigraphic position of primary volcanoclastic deposits within the eruptive sequence as a whole is variable from section to section. Variability is probably related to the distance to the nearest eruptive centre(s)

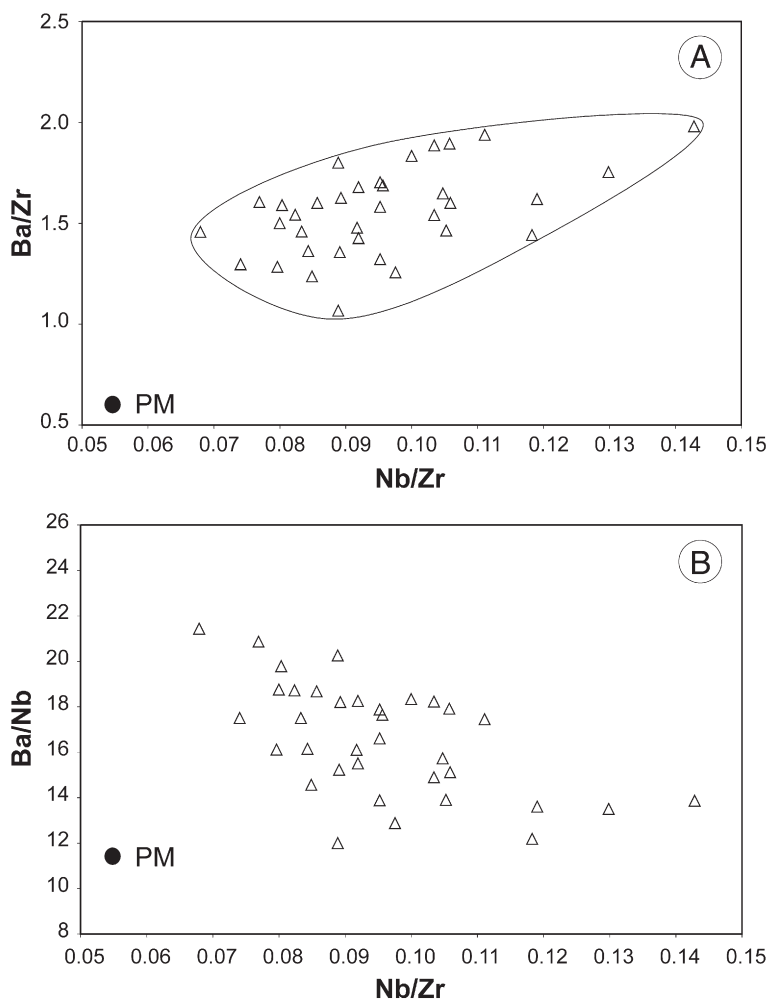


Fig. 8. Nb/Zr vs. Ba/Zr (A) and Nb/Zr vs. Ba/Nb (B) relationships in Algarve tholeiitic rocks. PM — primitive mantle ratios (Palme and O'Neil, 2003).

and/or direction of transport of volcaniclasts by eruptive or sedimentary processes, and location of unconsolidated sedimentary deposits allowing the formation of peperites. Volcaniclastic units may be in the upper part of the volcanic succession (Querença, Corcitos, Torre), at the base (Ayamonte), or intercalated throughout the sequence (Soidos). It is not possible to correlate lava flows or volcaniclastic deposits from section to section; even when in similar position in the sequence, volcanic units (lava flow or volcaniclastic deposit) may correspond to different eruptive events in different sections.

#### 3.4. Contemporaneous volcanism, sedimentation and erosion

Sediments are always present underlying, interbedded, or overlying the volcanic sequence (Fig. 2).

Contemporaneous sediments are: commonly red (locally light grey) mudstones (Fig. 3-E); lapilli or lapilli–breccia tuffites; conglomerate breccias, probably representing alluvial fans exemplified by the Ayamonte section (Fig. 3-J); and lahars at Corcitos. Caliche (calcareous soil) horizons developed in the Corcitos section are interpreted as paleosols developed on lava flows; these horizons represent intervals of volcanic quiescence in a semiarid climate.

Surface (lakes, ponds, shallow marine areas) or subsurface water bodies were likely present. Evidence is deduced from the abundance of peperite and/or hydromagmatic deposits (Torre, Soidos, Cabeço dos Passarinhos, Querença, Corcitos). Load casts and ball and pillow structures formed where lavas flowed over soft sediments (Torre, S. Bartolomeu de Messines, Querença, Corcitos, Soidos; Figs. 3-B, C and 4), magma intruding unconsolidated wet sediments (Cerro

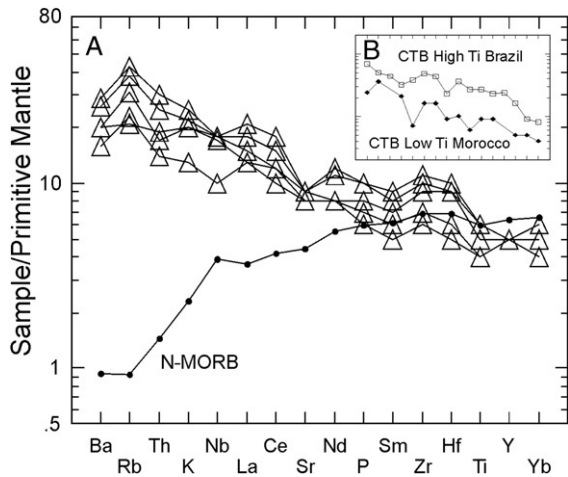


Fig. 9. Primitive mantle-normalized (Palme and O'Neil, 2003) incompatible trace elements abundances of the Algarve tholeiites. N-MORB values from Sun and McDonough (1989). Comparative continental CAMP tholeiitic basalts (CTB) from: Brazil High-Ti (De Min et al., 2003) and Morocco Low-Ti (Youbi et al., 2003).

dos Passarinhos, Cabeças–Silves; Fig. 5), and clay sediments injected upwards into extensional faults cutting the volcanic sequence (Corcitos, S, Bartolomeu de Messines; Fig. 3-I) represent magma interaction with coeval sedimentation. The thickness of the

sediments intercalated in effusive units is variable; they can be several metres thick to a few centimetres.

Erosive processes are also coeval with CAMP volcanism (before, during, and after). Evidence for erosion predating, or at the onset of, volcanic activity is given by two types of situation: by lava flows resting directly on erosion surfaces incised into the Silves Sandstones (Quinta da Ombria) or on Carboniferous slates and greywackes (Corcitos), or by large boulders of basaltic rock included in conglomerates at the base of the volcanic pile (Ayamonte). In listed sections, erosion surfaces cut the lava flows (Torre, Corcitos), or interbedded conglomerates that include fragments of lava eroded from other localities (Corcitos), prove the occurrence of erosion during the emplacement of the volcanic sequence. Subsequent erosion locally removed the upper part of the volcanic pile.

#### 4. Petrology and geochemistry

##### 4.1. Petrology, $P$ – $T$ conditions of magma fractionation

The analysed Lower Jurassic, rift-related, Algarve lava flows are characterized by well preserved magmatic textures and mineralogy, reflecting low degrees of weathering of the samples selected for this study.

Table 3

Representative major and trace element analyses of Lower Jurassic high-CaO rocks from the Algarve CAMP, with a subset of Sr-and O-isotope analyses (Martins, 1991)

Sample	R2-4	R2-31	R2-33	587-1	587-2	587-10	587-11	587-12	587-13	588-1
SiO <sub>2</sub> (wt.%)	48.93	47.10	47.43	47.25	45.67	49.69	49.11	49.47	50.44	48.11
TiO <sub>2</sub>	0.90	0.81	1.00	0.89	0.79	0.93	0.87	0.94	0.93	0.91
Al <sub>2</sub> O <sub>3</sub>	15.65	13.71	13.69	14.09	13.18	13.70	13.72	13.53	13.71	13.74
Fe <sub>2</sub> O <sub>3</sub> t	9.94	9.44	11.08	10.22	10.37	10.87	10.94	11.73	11.01	10.73
MnO	0.16	0.14	0.21	0.17	0.16	0.17	0.16	0.17	0.17	0.14
MgO	7.71	8.45	7.77	7.87	7.45	7.87	7.37	8.29	7.71	7.29
CaO	13.37	18.75	16.47	17.25	20.36	13.13	14.07	12.79	12.84	15.91
Na <sub>2</sub> O	1.62	1.70	2.02	2.02	1.28	2.60	2.63	2.42	2.35	2.35
K <sub>2</sub> O	0.60	0.17	0.46	0.45	0.40	0.73	0.62	0.50	0.56	0.80
P <sub>2</sub> O <sub>5</sub>	0.11	0.09	0.23	0.17	0.15	0.14	0.12	0.13	0.13	0.11
#Mg <sup>a</sup>	64.08	67.30	61.73	63.91	62.30	62.48	60.78	61.91	61.69	60.98
Sc (ppm)	36	38	32	36	35	32	32	34	33	36
V	252	218	245	238	214	260	250	259	256	236
Cr	213	182	165	185	160	220	209	209	217	190
Ni	87	86	83	76	85	95	106	88	98	52
Rb	9	4	15	6	4	21	7	12	23	7
Sr	481	724	742	792	1267	390	588	407	411	561
Y	22	23	26	28	20	23	25	25	23	22
Zr	84	63	90	87	90	83	79	92	82	89
Nb	9	8	10	11	14	9	n.d.	7	9	8
Ba	89	117	111	112	137	133	112	120	132	120
( <sup>87</sup> Sr/ <sup>86</sup> Sr) <sub>0</sub>		0.707380	0.707204	0.707290	0.707456	0.706811	0.707091	0.706805	0.706852	0.706995
δ <sup>18</sup> O (‰)				8.73	8.73	6.86	6.96	6.92	6.72	

<sup>a</sup> Mg# = 100 Mg/(Mg \* Fe<sup>2+</sup>); Fe<sup>3+</sup>/Fe<sup>2+</sup> = 0.15. <sup>b</sup> Initial ratio (<sup>87</sup>Sr/<sup>86</sup>Sr)<sub>0</sub> computed at 198 Ma (based on age of Verati et al., 2007).

Dominant textures are ophitic to subophitic, sometimes with a porphyritic tendency. Mineral assemblages, include: rare, partially reabsorbed olivine (Fo<sub>50–47</sub>); plagioclase (An<sub>80–75</sub>; microliths included in clinopyroxene; An<sub>80–25</sub>; individual laths); two clinopyroxenes (diopside/augite: Wo<sub>45–32</sub> En<sub>37–54</sub> Fs<sub>18–14</sub> and pigeonite: Wo<sub>8–11</sub> En<sub>67–56</sub> Fs<sub>25–33</sub>; Table 1); titanomagnetite (Usp<sub>60–40</sub>); ilmenite (Ilm<sub>98–94</sub>); with minor apatite and biotite, together with quartz-alkali feldspar (Or<sub>73–53</sub>) graphic intergrowths (Appendix B). The mineral assemblages and textures are characteristic of fractionated continental tholeiitic magmas.

The fractionation sequence was dominated by early crystallization of olivine+bytownite/labradorite+Cr-bearing (up to 0.5 wt.%) diopside, followed by olivine re-absorption and further crystallization of Fe-rich augite+pigeonite+labradorite/andesine+Fe–Ti oxides±apatite assemblages. At the latest stage of fractionation, minor biotite and quartz+K-feldspar intergrowths fill interstitial spaces.

From geothermometric estimates (cf. Putirka et al., 2003; Andersen et al., 1993) initial (Mg-rich) clinopyroxene crystallization was at 1230±20 °C, and augite–pigeonite equilibrium within the range of 1030±90 °C. Ti-magnetite+ilmenite equilibrium provides temperature estimates of 1020 °C to 730 °C, suggesting  $fO_2$

conditions more reduced than those of the QFM buffer [ $\Delta \log(fO_2)_{QFM} = -1.7$  to  $-0.4$ ]. Clinopyroxene-liquid geobarometry (cf. Putirka et al., 2003) indicates that the main fractionation occurred at an average depth of 26±4 km ( $P = 0.69 \pm 0.11$  GPa), consistent with extensive magma underplating at the SW Iberia Variscan crust/mantle boundary, which is estimated to have been located at about 30 km depth pre-rifting (Stapel et al., 1996). Further magmatic differentiation occurred during short-term residence within shallow level crustal magma chambers as discussed below.

#### 4.2. Geochemical magma characterization

Low alkalis content for a given SiO<sub>2</sub> is consistent with a subalkaline character of the Algarve Lower Jurassic lavas (Fig. 6 and Table 2). This result is supported by their CIPW normative compositions, mostly comprising hypersthene–quartz and hypersthene–olivine associations. Tholeiitic affinity and low TiO<sub>2</sub> contents (0.75–1.20 wt.%) demonstrates commonality with Low-Ti tholeiites characteristic of CAMP basalts elsewhere (e.g. Bertrand et al. 1982; Cox, 1988; Nomade et al., 2002; De Min et al., 2003).

The geochemistry of the Algarve tholeiitic basalts (Mg#: 59–71; MgO<10 wt.%; Ni<110ppm and

588-2	597-16	597-18	597-19	597-20	E2-4	E3-1	E5-1
47.94	48.58	50.18	50.39	50.50	45.98	48.86	49.09
0.89	0.87	1.01	0.86	0.88	0.80	0.86	0.80
13.19	13.72	13.96	13.70	13.53	12.93	13.70	15.60
9.94	10.29	10.72	10.73	10.84	9.58	10.29	11.08
0.16	0.17	0.20	0.18	0.19	0.13	0.14	0.17
8.69	6.87	7.04	7.87	7.45	7.46	7.71	7.95
16.23	16.55	13.60	13.18	13.61	20.40	15.51	13.37
2.42	2.44	2.29	2.32	2.35	2.16	2.09	1.56
0.60	0.49	0.61	0.56	0.63	0.26	0.44	0.66
0.09	0.14	0.14	0.10	0.11	0.12	0.14	0.12
66.79	60.56	60.17	62.78	61.25	64.17	63.28	62.27
37	34	33	38	38	33	32	33
259	245	263	270	266	206	250	228
212	202	217	231	225	177	198	221
90	78	92	88	101	78	79	75
7	4	38	21	14	1	12	16
708	733	359	387	389	1224	765	755
22	19	26	21	23	27	21	24
92	87	94	82	82	146	71	75
8	9	9	8	10	14	4	9
137	112	126	100	107	130	133	-
	0.707281	0.706645	0.706740	0.706757	0.707403	0.707310	
		7.51	7.95	8.10	7.66		

Cr < 240 ppm) clearly indicates that they are not representative of primary magmas, in agreement with the petrographic evidence described above. Based on Ni–K and Ni–Zr relationships (Fig. 7), and variable incompatible element ratios (Fig. 8), the observed compositional spectrum may best be explained mainly in terms of partial melting of heterogeneous mantle sources, followed by extensive fractional crystallization of distinct primary magmas.

Rare earth elements (REE) display coherent fractionation, where  $(La/Yb)_N = 3.03–3.43$ . Typical geochemical characteristics of Algarve basalts include: (1) significant enrichment in large ion lithophile elements (LILE: Rb, Ba, K, Th) and light REE relative to high field strength elements (HFSE: Nb, Ta, Zr, Hf, Ti, Y) and heavy REE; (2) moderately high initial Sr ( $(^{87}Sr/^{86}Sr)_0 > 0.7050$ ) and oxygen ( $\delta^{18}O > +7.40\%$ ) isotope ratios; and (3) negative anomalies of Nb (Ta), Sr, P and Ti (Appendix B; Fig. 9; Table 2).

Collectively, these geochemical features could be interpreted either as the result of partial melting of heterogeneous continental lithospheric mantle (CLM), previously affected by Variscan suprasubduction metasomatic events, or as a consequence of continental crust contamination of mantle magmas. However, the observed variation trends between incompatible HFSE and LILE ratios (Fig. 8) cannot be exclusively reconciled with simple crustal contamination and/or AFC (DePaolo, 1981) processes. Specifically, the decrease of Ba/Nb ratios (trending towards typical primitive mantle values; Fig. 8B) with increasing Nb/Zr (an index of “within-plate” mantle source enrichment) strongly suggest the interaction of different mantle source components during the genesis of Algarve magmas. Therefore, we argue that the main geochemical characteristics of Algarve magmas reflect the complex evolution of their mantle sources, where melting of older orogenic lithospheric mantle (CLM) was progressively superimposed by introduction of new asthenospheric (upper mantle and/or deeper plume) components during the initial stages of continental rifting magmatism.

Initial Sr-isotope ratios and  $\delta^{18}O$  signatures of Algarve tholeiites are higher than those typical of basalts sourced in lithospheric mantle (cf. Wilson and Downes, 1991; Faure and Mansing, 2005). As well, relationships between Ni–K contents and  $(^{87}Sr/^{86}Sr)_0 - ^{18}O/^{16}O$  isotope ratios (Fig. 7), are consistent with coupled crustal assimilation/fractional crystallization (AFC; DePaolo, 1981) also contributing to the chemical variability of the lavas (see also Youbi et al., 2003). This inferred AFC likely occurred in magma

chambers close to the crust/mantle boundary, from density considerations, as endorsed by estimates of 26 km from clinopyroxene-liquid geobarometry.

Evidence for significant carbonate contamination discussed below, and the rare occurrence of silicate crustal xenoliths, suggests that during ascent magmas also interacted with mid and upper continental crust, most likely contributing to the assimilation of low solidus crustal materials.

Incompatible multi-element patterns are similar to typical continental tholeiites elsewhere, specifically tholeiites occurring in the neighbouring contemporaneous Moroccan CAMP province (e.g. Bertrand et al. 1982; Youbi et al., 2003; Fig. 9). In addition to eruptive sequences in the Algarve, the CAMP in Iberia also comprises the Messejana Dike and the Santiago do Cacém Basin lava flows (Fig. 1). Comparison of our data with the results of Cébria et al. (2003) and Youbi et al. (2003) indicates a commonality of mineralogical and geochemical characteristics for all those magmatic suites.

#### 4.3. Evidence for carbonate assimilation

Detailed outcrop observation at several localities (e.g. Alte, Querença, Soidos), provides evidence for the development of (mesoscale) domainal lithological heterogeneities within lava flows. Heterogeneities are defined where typical greyish, medium/fine grained (sub) ophitic facies rocks gives way to greenish, very fine-grained porphyritic counterparts; fine-grained (porphyritic) domains may either correspond to whole lava flow units or to mesoscale heterogeneities within a given flow.

These rock domains are also characterized by a distinct geochemistry (Table 3). Lower SiO<sub>2</sub> abundances (45.67 to 50.00 wt.%) yield an highly SiO<sub>2</sub> undersaturated character with up to 10.03 wt.% normative nepheline and 1.22 wt.% normative leucite. Contents of CaO and Sr (12.5 to 20.4 wt.% and 235 to 1337 ppm, respectively), and  $(^{87}Sr/^{86}Sr)_0$  isotope ratios (0.70665 to 0.70746) are high when compared with respective values in the dominant ophitic/subophitic facies rocks (SiO<sub>2</sub> = 50–53 wt.%; CaO = 9–12 wt.%; Sr = 149–233 ppm;  $(^{87}Sr/^{86}Sr)_0 = 0.70539–0.70634$ ).

As expected, observed geochemical contrasts correspond to distinct mineral assemblages. High-CaO (finer-grained porphyritic facies) rocks comprise phenocrysts of plagioclase (An<sub>81</sub>), olivine (Fo<sub>62</sub>) and clinopyroxene (endiopside-augite cores – Wo<sub>41</sub> En<sub>50</sub> Fs<sub>9</sub>, SiO<sub>2</sub> = 53 wt.%, Al<sub>2</sub>O<sub>3</sub> = 2.65 wt.%, rimmed by Ca–Al-rich clinopyroxene – Wo<sub>53</sub> En<sub>30</sub> Fs<sub>17</sub>, SiO<sub>2</sub> = 47 wt.%, Al<sub>2</sub>O<sub>3</sub> = 9.1 wt.%; Table 1). These are set into

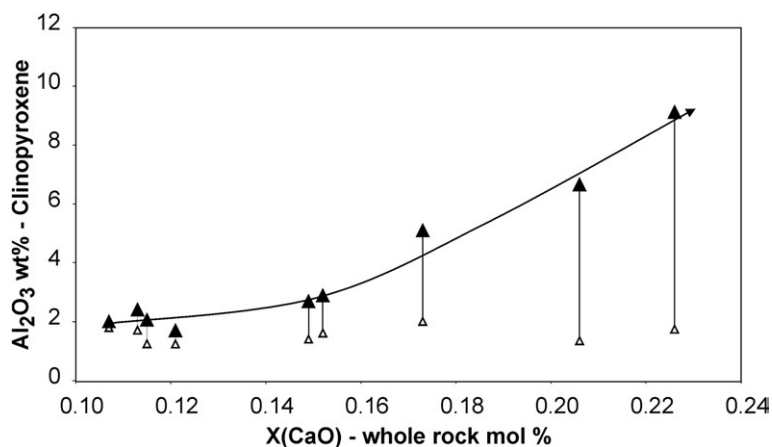


Fig. 10. Variations of  $\text{Al}_2\text{O}_3$  wt.% clinopyroxene–whole rock  $X(\text{CaO})_{\text{molar}}$  fraction in basalts (minimum and maximum  $\text{Al}_2\text{O}_3$  wt.% clinopyroxene contents in individual samples are connected by straight lines; see Table 1). Increasing (maximum) clinopyroxene  $\text{Al}_2\text{O}_3$  contents in “high-Ca ( $X(\text{CaO}) \geq 0.12$ ) porphyritic facies domains”, Ca-plagioclase bearing, rock domains indicates decreasing  $a_{\text{SiO}_2}$  in their respective melts [ $\text{CaAlAlSiO}_2^{\text{cpx}} + \text{SiO}_2^{\text{melt}} = \text{CaAl}_2\text{SiO}_8^{\text{plag}}$ ; see paragraph 4.3].

a very fine granular matrix, which also includes (Ca, Al-rich) clinopyroxene, plagioclase ( $\text{An}_{70-43}$ ), olivine ( $\text{Fo}_{48}$ ) and Ti-magnetite. Enrichment of  $\text{Al}_2\text{O}_3$  in clinopyroxenes (reflecting extensive incorporation of Ca-Tschermak component) correlates with increasing CaO contents of their host rocks (Fig. 10), being consistent with the remaining mineralogical/geochemical data which indicate a significant decrease of  $a_{\text{SiO}_2}^{\text{melt}}$  in the high-CaO domains relative to the typical  $\text{SiO}_2$  saturated character of the dominant tholeiitic magmas.

From Fig. 11, decreasing  $\text{SiO}_2/\text{CaO}$  ratios in “porphyritic rock domains” should reflect variable

mixing of Algarve tholeiitic magmas with a  $\text{SiO}_2$ -poor, CaO-rich component (see Vollmer, 1976; Langmuir et al., 1978). Other companion plots (involving elements and isotopes; Figs. 12 and 13) also comply with binary mixing curves, where individual samples maintain the same relative relationship to one another on all plots, substantiating the mixing process (cf. Langmuir et al., 1978). Given the inferred major element characteristics of end-members (Fig. 11), adequate representatives of the high-Ca,  $\text{SiO}_2$ -poor end-member could have been derived from magmatic assimilation (and subsequent decarbonation/mixing) of calcitic–carbonates.

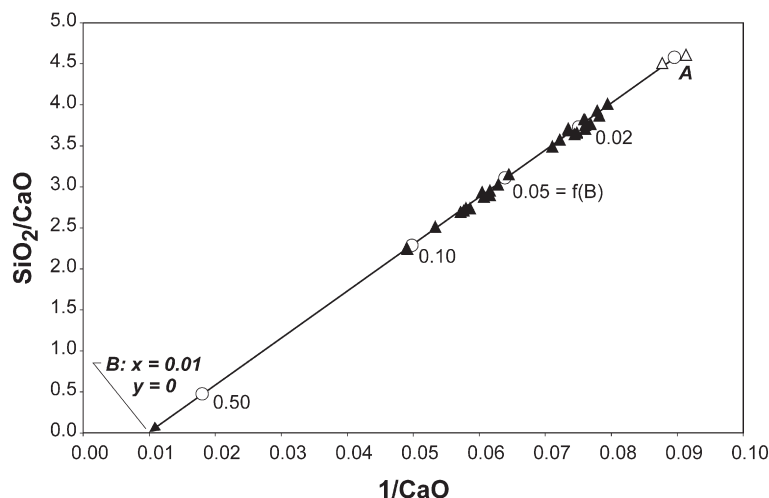


Fig. 11.  $\text{SiO}_2/\text{CaO}$ – $1/\text{CaO}$  diagram substantiating the hypothesis for development of “high-Ca, porphyritic rock domains” through binary mixing of Algarve tholeiitic magmas (component A:  $x = 0.089$ ,  $y = 4.56$ ) and a  $\text{SiO}_2$ -poor, CaO-rich (B) carbonate derived component (text Section 4.3). ( $f(\text{B})$  = fraction of end-member, component B in the mixture). Higher  $f(\text{B})$  values ( $\sim 0.1$ ) should correspond to about 18–20% carbonate assimilation.

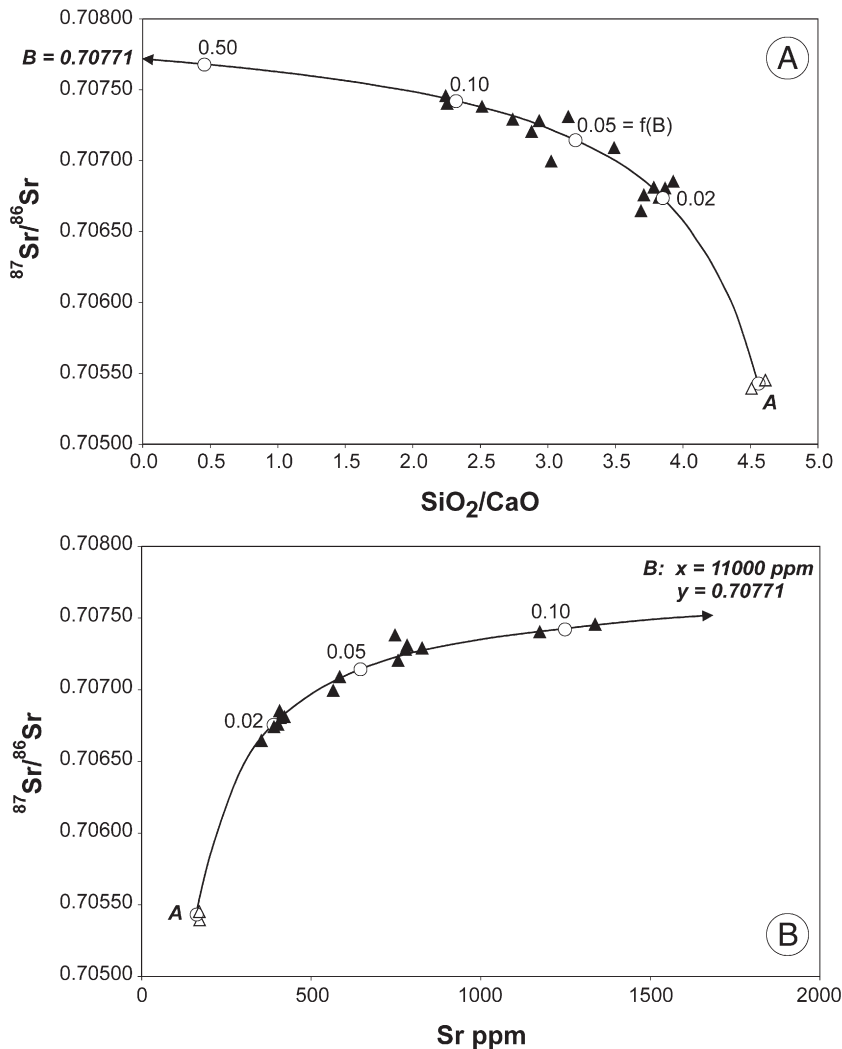


Fig. 12.  $(^{87}\text{Sr}/^{86}\text{Sr})_0$ - $\text{SiO}_2/\text{CaO}$  (A) and  $(^{87}\text{Sr}/^{86}\text{Sr})_0$ -Sr (ppm) (B) diagrams illustrating chemical and isotope variations associated with binary mixing in tholeiitic magmas. ( $f(B)$ =fraction of component B in the mixture; component A:  $x$ - $\text{SiO}_2/\text{CaO}=4.56$ , Sr=171 ppm,  $y=0.70542$  — average of less radiogenic, non-contaminated, Algarve tholeiites; see Table 2). Maximum Sr contents inferred for (oxide-MO) component B corresponds to about 6200 ppm strontium in the original assimilated carbonates.

Notwithstanding the complex chemical processes inherent to carbonate assimilation by silicate magmas, analysis of appropriate mixing equations (Vollmer, 1976; Langmuir et al., 1978) indicates that the compositional range of high-CaO “porphyritic rock” is compatible with mixing of Algarve tholeiite magmas with  $\sim 2$ – $10\%$  of an almost pure Ca-carbonate component (see Fig. 11). Such lithologies are present in the Paleozoic basement, below the lower-Mesozoic Algarve basin.

On this basis, the assimilated carbonates are inferred to have had high Sr contents (Sr  $\sim 6200$  ppm) and relatively high  $\delta^{18}\text{O}$  ( $\sim +23\%$  to  $+25\%$ ) and  $(^{87}\text{Sr}/^{86}\text{Sr})_0$

( $\sim 0.70771$ ) isotope ratios (Figs. 12 and 13; Appendix B). Such values are consistent with Viséan, shallow water (platform) marine carbonates (Sr=2000–9000 ppm,  $\delta^{18}\text{O}=26.8\pm 2.5\%$ ,  $(^{87}\text{Sr}/^{86}\text{Sr})_0 \sim 0.70771$ ; see, Schlanger, 1985; Veizer et al., 1999; McArthur et al., 2001; Veizer, 2004) that comprise the Murração and Quebradas units of the Bordeira Formation (Manuppella, 1992), outcropping at the SW corner of the South Portuguese Zone Paleozoic basement.

Carbonate-contaminated and uncontaminated lava flows coexist and alternate in the same sequence. Carbonate-contamination is always expressed by the occurrence of very fine-grained porphyritic textures,

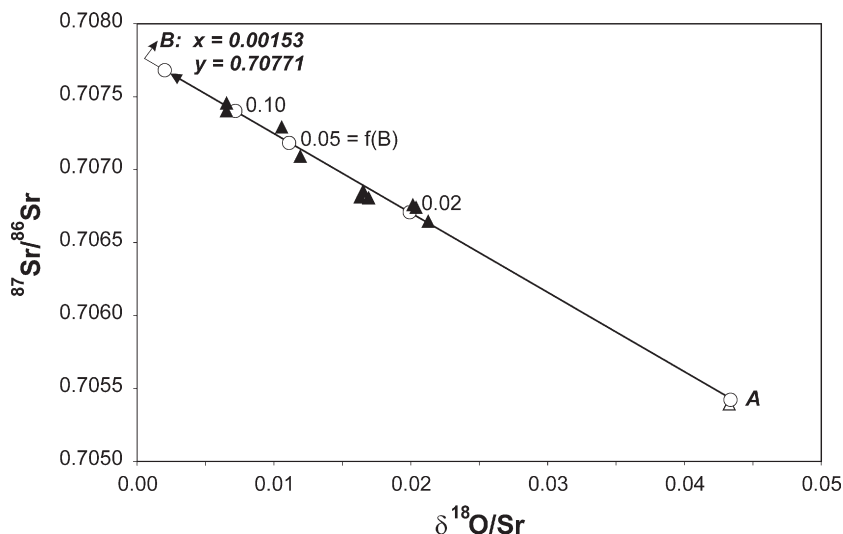


Fig. 13.  $(^{87}\text{Sr}/^{86}\text{Sr})_0$ – $\delta^{18}\text{O}/\text{Sr}$  diagram illustrating strontium and oxygen isotope variations associated with mixing processes in Algarve magmas ( $f(\text{B})$ =fraction of component B in the mixture; component A:  $x=0.04327$ ,  $y=0.70542$  — non-contaminated, least radiogenic, lowest  $\delta^{18}\text{O}$  ( $\sim+7.40\%$ ), Algarve tholeiite; see Table 2). Assuming a  $\delta^{18}\text{O}$  fractionation of  $-6\%$  to  $-8\%$  during decarbonation (Valley, 1986), the inferred  $\delta^{18}\text{O}$  ( $\sim+17\%$ ) value for (oxide–MO), end-member component B, should translate into  $\delta^{18}\text{O} \sim +23$ – $+25\%$  in the original assimilated carbonates.

whereas the predominant uncontaminated lavas have dominant ophitic to subophitic texture. This textural difference is consistent with devolatilization of magma domains where carbonate digestion occurred. Assimilation of carbonates by silicate magmas produces  $\text{CO}_2$ , which has limited solubility in tholeiitic magmas at low to moderate pressure (e.g. Dixon, 1997; Lowenstern, 2000). The effect of  $\text{CO}_2$  on lowering the liquidus temperature of magmas, as well as the abrupt changes in magma liquidus temperature by volatile loss is well known (e.g. Westrich et al., 1988; Hort, 1998; Barnes et al., 2005). Thus, significant undercooling by  $\text{CO}_2$  loss may have induced an increase in crystal nucleation rates, which determined the crystal size and produced the fine-grained textures that characterize the carbonate-contaminated rocks.

## 5. Discussion and conclusions

### 5.1. Paleogeography and facies model

The characteristics of the volcanic and sedimentary deposits, and erosion surfaces, are consistent with a facies model typical of continental basaltic successions (cf. Cas and Wright, 1987). The paleogeographic setting would be that of a mountain-and-basin morphology, in semi arid climatic conditions, with the basins receiving clastic sedimentation from elevated regions coeval with volcanism. Alluvial fans would have been deposited at the

base of fault scarps, whereas finer facies of sands, silts, clays, carbonates and evaporites were located distally from the up-thrown blocks, depending on the size of the basins.

Endorheic torrential fluvial systems, ponded by lava flows, would create lakes or swampy areas. These would collect sandy/clayey sediments (including remobilised pyroclastic particles) and pyroclastic fall deposits. Lava flowing over unconsolidated sediments would partially sink into it, resulting in convoluted/pillowed lava flow bases or magma completely intruding the sediment. Explosive water-magma interaction and wet sediment/magma mingling would be a common characteristic of such depositional environment. Hydro-magmatic pyroclastic deposits and peperite would then be produced, containing abundant lithic fragments from the underlying sequences. In these conditions, eruptive centres would predominantly be maars or tuff rings. Such structures are not easy to identify in cross section in limited outcrops, and, thus, have not been recognised yet.

Areas uplifted by contemporaneous tectonics could explain erosion surfaces over which volcanic sequences directly overly the Silves Sandstones or the Carboniferous basement, as in the Quinta da Ombria and Corcitos areas. On the other hand, paleosols (caliche) developed on top of lava flows reflect relatively long periods of weathering between short duration volcanic episodes.

## 5.2. Mantle plume or passive rifting

Lower Jurassic Algarve basalts present characteristics, which enable its inclusion in the low-Ti basalts described for some large igneous provinces. These magmatic provinces may feature both low-, and high-Ti basalts, typically with different geographic distributions. The two groups cannot be related by fractional crystallization, requiring different mantle sources. Low-Ti basalts do not occur in oceanic LIP (Hawkesworth et al., 2000), consistent with the continental setting of the Algarve CAMP sector.

Continental rifting is a complex process resulting from a tensional stress field caused by sublithospheric mantle dynamics or, alternatively, arising from far-field horizontal forces related to plate kinematics. Sengor and Burke (1978) termed these end-members active and passive rifts, respectively. In active rifts, magmatism is considered a direct product of a mantle plume melting, or of lithospheric melting induced by the impingement of the plume on the base of the lithosphere. In passive models, magmatism results from adiabatic decompression of the asthenosphere and/or lithosphere induced by lithospheric extension and thinning. Formation of the Central Atlantic rift, and other continental dispersals, has been the locus of an intense debate between those proposing a passive rift model (e.g. McHone, 2000; Sears et al., 2005; Verati et al., 2005) and those defending a mantle plume as the triggering rift mechanism (e.g. Wilson, 1997; Oyarzun et al., 1997).

The distinction between these two types of rifting is not easy given that both may produce similar geological and geophysical signatures (Ruppel, 1995; Ionov, 2002). Moreover, considering that some of the main lines of evidences for passive or active rifting are dynamic (e.g. heat flow) distinguishing between these models is not readily tractable when dealing with  $\approx 200$ Ma old events.

Algarve CAMP magmatism cannot be the direct result of plume melting. Given a pre-rift Variscan lithosphere (CLM) thickness of about 125 km (Stapel et al., 1996) and that lithosphere limits the adiabatic ascent of plumes (e.g. Lassiter and DePaolo, 1997), that CLM would constrain the plume melting to depths with residual garnet, which is incompatible with the genesis of the Algarve tholeiites. However the role of a mantle plume as inductor of the Algarve magmatism cannot be immediately discarded given that plumes can cause lithospheric fusion. This question is further addressed below.

Active rifting in response to an ascending mantle plume is characterized by important doming/uplift pre-

ceding volcanism and radial depositional features (Rainbird and Ernst, 2001). In contrast, initial stages of passive rifting, being caused by lithospheric stretching driven by far-field horizontal plate forces, are marked by tectonic subsidence and sedimentation (e.g. Turcotte and Emermam, 1983; Bédard, 1985). In the Algarve Basin Lower Jurassic sedimentation starts with continental clastic deposits and becomes progressively deeper in agreement with a subsiding environment. The Carnian (228.0 to 216.5 Ma) or pre-Carnian age attributed to the beginning of sedimentation based on paleontological evidence (Palain, 1979; Manuppella, 1988, 1992) indicates that magmatism followed some 20 to 30Ma later. The time difference between the inception of sedimentation and magmatism is strongly suggestive that the driving force of the Algarve lower Mesozoic rifting was of the passive type.

The existence of thickened lithosphere inherited from the Hercynian orogeny, causing a significant reduction of lithosphere strength (e.g. Kuszniir and Park, 1987; Dunbar and Sawyer, 1989), is here considered to have favoured continental rifting. The location of rifting may have been determined by pre-existing plate mechanical anisotropies (see Sheth, 1999). Algarve Basin formed in relation with a left-lateral transtensional zone, accommodating the differential movement of Africa with respect to Eurasia (e.g. Klitgord and Schouten, 1986; Terrinha et al., 2002). This Lower Jurassic through Late Cretaceous transtensive shear zone (Newfoundland-Gibraltar Fracture Zone) was inherited from Variscan times during which it acted as a dextral transpressive strike-slip boundary (Keppie, 1989). These features suggest that a pre-existing zone of weakness controlled the location of the Algarve rift basin (see also Mata et al., 2006). They also point to the probable role of inherited lattice preferred orientation of mantle lithospheric olivine, which induced mantle mechanical anisotropy constraining strain localization (see Tommasi and Vauchez, 2001).

Lower Jurassic Algarve CAMP magmatism was recently dated by the  $^{40}\text{Ar}/^{39}\text{Ar}$  method at  $198.1 \pm 1.6$  to  $198.4 \pm 2.8$ Ma (Verati et al. 2007), being almost coincident with the ages reported for the CAMP major volcanic pulse, elsewhere (Marzoli et al., 2004; Knight et al., 2004; Verati et al., 2005; 2007; Nomade et al., 2007). From our data, a passive rifting model seems most appropriate to explain the rifting preserved in the Algarve volcanostratigraphic sequence. However, the extension of this model to the CAMP as a whole seems to be more problematic given the short duration ( $\approx 1.5$  Ma) of the magmatic peak activity over circa

$7 \times 10^6 \text{ km}^2$ , which is also not easy to explain by a single mantle plume (e.g. Olsen, 1999).

A source of the tholeiites in continental lithosphere, by decompressional melting during extension, is also in keeping with passive rifting. Geochemical data indicating progressive inputs of basalt melts from an asthenospheric source, either upper mantle or a plume originating at deeper levels, tracks progressive opening of an ocean. Accordingly, different sectors of Pangean rifting in the North Atlantic may have been passive or active.

## Acknowledgements

Financial support for this work was provided by a bilateral co-operation project between CNRST (Morocco) and GRICES (Portugal) to L.T.M., J.M., N.Y and J.M.M. This study is a contribution to research projects POCA-PETROLOG (Centro de Geologia Univ. Lisboa, UI: 263; POCTI/FEDER) and GEODYN (LATTEX, POCTI-ISFL-5-32). Funding for the O and Sr-isotope analysis was provided by an NSERC research grant to R. Kerrich. A. Marzoli and two anonymous reviewers are acknowledged by their incisive and constructive comments. We thank Jarda Dostal and John Greenough for organizing this special issue of *Lithos*, and C. Mourão for typing and drafting assistance.

## Appendix A. Location of specified sections and outcrops

Section/outcrop	N latitude	W longitude	Altitude*
Cabeças-Silves	37° 12' 09"	8° 24' 49"	65
Torre (base)	37° 14' 29"	8° 19' 59"	160
Torre (top)	37° 14' 25"	8° 19' 43"	180
S. Bartolomeu de Messines	37° 15' 00"	8° 16' 58"	166
Soidos (base)	37° 14' 54"	8° 11' 01"	268
Soidos (top)	37° 15' 15"	8° 09' 27"	425
Cerro dos Passarinhos	37° 12' 47"	8° 01' 57"	260
Quinta da Ombria	37° 11' 39"	8° 00' 49"	133
Corcitos (top)	37° 13' 09"	7° 59' 45"	250
Corcitos (base)	37° 13' 04"	7° 59' 18"	206
Querença (top)	37° 11' 52"	7° 58' 52"	211
Querença (base)	37° 12' 10"	7° 58' 51"	200
Ayamonte	37° 13' 49"	7° 24' 05"	30

GPS coordinates in DMS format, referred to WGS84; \*Metres above sea level.

## Appendix B. Analytical methods

### B.1. Electron microprobe

Mineral phases (olivines, clinopyroxenes, plagioclase and oxides) were analysed at University of Lisbon (Centro de Geologia) using a Geol JXA 733<sup>®</sup> microprobe

operating with a 5 $\mu\text{m}$  beam diameter at 15kv to 18kv and 15nA. Synthetic metals (Cr, V and Ni) and natural minerals (for all others elements) were used as standards. Precision is better than 2% for major elements. Analytical procedures as in Munhá (1981).

### B.2. Major and trace element analyses

Major and trace element analyses were performed at University of Lisbon (Department of Geology). SiO<sub>2</sub> was analysed gravimetrically, and other major elements were determined by Atomic Absorption Spectrometry (AAS) using a Perkin Elmer 403 AAS. The major elements Ti and P and the trace elements Sc, V, Cr, Ni, Sr, Rb, Y, Zr, Nb and Ba were analysed in pressed pellets by X-Ray fluorescence spectrometry using a Philips PW 1410/00 instrument. Based on the use of International Reference Materials, including BCR-2, the accuracy was estimated at 2% for SiO<sub>2</sub>, 10% for the other major elements and 5% for trace elements. Precision was estimated from replicate analyses.

Procedures for analysis of major elements, and selected trace elements (Sc, V, Cr, Ni, Sr, Rb, Y, Zr, Nb and Ba) by X-ray fluorescence spectrometry (XRF) at University of Lisbon are given by Munhá (1981).

Rare Earth Elements, Hf and Th were determined by instrumental neutron activation analysis (INAA) by Nuclear Activation Services (Canada). The accuracy of analyses was evaluated by analysing the United States Geological Survey standard basalt BHVO-1 as unknown; the errors were generally less than 10%, with results for many elements within  $\pm 5\%$  of recommended values.

### B.3. Stable and radiogenic isotope analyses

Oxygen was extracted from whole rock samples with BrF<sub>5</sub> at 600–650 °C, and then converted to CO<sub>2</sub>, prior to mass spectrometric analysis using a Micromass 602. Results are reported as  $\delta^{18}\text{O}$ -values in ‰ relative to the V-SMOW (Vienna Standard Mean Ocean Water). Whole rock analyses are reproducible to  $\pm 0.2\%$ . The  $\delta^{18}\text{O}$ -value determined for NBS 28 Quartz Standard is +9.6‰. Procedures as in Feng et al. (1993).

Strontium was separated by standard cation-exchange methods using teflon<sup>®</sup>-HDEHP. Routine total procedure blanks were Sr < 1 ng. Radiogenic isotope analyses were done using a Finnigan MAT 261<sup>®</sup>. Sr-isotope ratios are normalized to  $^{86}\text{Sr}/^{88}\text{Sr} = 0.1194$  and relative to  $^{87}\text{Sr}/^{86}\text{Sr} = 0.710234 \pm 0.000003$  ( $2\sigma$ ;  $n = 88$ ) in NBS 987. The external precision ( $2\sigma$ ) is better than  $\pm 3.5 \times 10^{-5}$ . For Sr-isotope analyses, rock powders were leached in 6N HCl. Procedures as in Mata et al. (1998).

## References

- Alibert, C., 1984. A Sr–Nd isotope and REE study of late Triassic dolerites from the Pyrenees (France) and the Messejana Dyke (Spain and Portugal). *Earth and Planetary Science Letters* 73 (1), 81–90.
- Andersen, D.J., Lindsley, D.H., Davidson, P.M., 1993. QUILF: a Pascal program to assess equilibria among Fe–Mg–Mn–Ti oxides, pyroxenes, olivine, and quartz. *Computers and Geosciences* 19 (9), 1333–1350.
- Barnes, C.G., Prestvik, T., Sundvoll, B., Surrat, D., 2005. Pervasive assimilation of carbonate and silicate rocks in the Hortavaer igneous complex, north-central Norway. *Lithos* 80, 179–199.
- Bédard, J.H., 1985. The opening of the Atlantic, the Mesozoic New England igneous province, and mechanisms of continental breakup. *Tectonophysics* 113, 209–232.
- Bertrand, H., Dostal, J., Dupuy, C., 1982. Geochemistry of early Mesozoic tholeiites from Morocco. *Earth and Planetary Science Letters* 58 (2), 225–239.
- Cas, R.A.F., Wright, J.V., 1987. *Volcanic Successions: Modern and Ancient*. Chapman and Hall, London. 528 pp.
- Cebriá, J.M., López-Ruiz, J., Doblas, M., Martins, L.T., Munhá, J., 2003. Geochemistry of the Early Jurassic Messejana–Plasencia dyke (Portugal–Spain); Implications on the origin of the Central Atlantic Magmatic Province. *Journal of Petrology* 44, 547–568.
- Cox, K.G., 1988. The Karoo Province. In: Macdougall, J.D. (Ed.), *Continental Flood Basalts*. Kluwer Academic Publishers, pp. 239–271.
- De Min, A., Piccirillo, E.M., Marzoli, A., Bellieni, G., Renne, P.R., Ernesto, M., Marques, L.S., 2003. The Central Atlantic Magmatic Province (CAMP) in Brazil: petrology, geochemistry,  $40\text{Ar}/39\text{Ar}$ , paleomagnetism and geodynamic implications. In: Hames, W.E., McHone, J.G., Renne, P.R., Ruppel, C. (Eds.), *The Central Atlantic Magmatic Province: Insights From Fragments of Pangea*. Geophysical Monographs Series, vol. 136. American Geophysical Union, pp. 91–128. doi:10.1029/136GM06.
- DePaolo, D.J., 1981. Trace element and isotopic effects of combined wallrock assimilation and fractional crystallization. *Earth and Planetary Science Letters* 53, 189–202.
- Dixon, J.E., 1997. Degassing of alkaline basalts. *American Mineralogist* 82, 368–378.
- Dunbar, J.A., Sawyer, D.S., 1989. How pre-existing weaknesses control the style of continental breakup. *Journal of Geophysical Research* 94, 7278–7292.
- Dunn, A.M., Reynolds, P.H., Clarke, D.B., Ugidos, J.M., 1998. A comparison of the age and composition of the Shelburne dyke, Nova Scotia, and the Messejana dyke, Spain. *Canadian Journal of Earth Sciences* 35, 1110–1115.
- El Arabi, E.H., Bienvenido Diez, J., Broutin, J., Essamoud, R., 2006. Première caractérisation palynologique du Trias moyen dans le Haut Atlas; implications pour l'initiation du rifting téthysien au Maroc. *Comptes Rendus de Géoscience* 338, 641–649.
- Faure, G., Mensing, T.M., 2005. *Isotope geology: principles and applications*, 3rd edition. John Wiley & Sons, Hoboken, N.J. 928 pp.
- Feng, R., Kerrich, R., Maas, R., 1993. Geochemical, oxygen, and neodymium isotope compositions of metasediments from the Abitibi greenstone belt and Pontiac Subprovince, Canada: evidence for ancient crust and Archean terrane juxtaposition. *Geochimica et Cosmochimica Acta* 57 (3), 641–658.
- Gradstein, F.M., Ogg, J.G., Smith, A.G., Agterberg, F.P., Bleeker, W., Cooper, R.A., Davydov, V., Gibbard, P., Hinnov, L.A., House, M.R., Lourens, L., Luterbacher, H.P., McArthur, J., Melchin, M.J., Robb, L.J., Shergold, J., Villeneuve, M., Wardlaw, B.R., Ali, J., Brinkhuis, H., Hilgen, F.J., Hooker, J., Howarth, R.J., Knoll, A.H., Laskar, J., Monechi, S., Plumb, K.A., Powell, J., Raffi, I., Röhl, U., Sadler, P., Sanfilippo, A., Schmitz, B., Shackleton, N.J., Shields, G.A., Strauss, H., Van Dam, J., van Kolfshoten, T., Veizer, J., Wilson, D., 2004. *A Geologic Time Scale 2004*. Cambridge University Press. 589 pp.
- Hawkesworth, C.J., Gallagher, K., Kirstein, L., Mantovani, M.S.M., Peate, D.W., Turner, S.P., 2000. Tectonic controls on magmatism associated with continental break-up. *Earth and Planetary Science Letters* 179 (2), 335–349.
- Head III, J.W., Coffin, M.F., 1997. Large igneous provinces: a planetary perspective. In: Mahoney, J.J., Coffin, M.F. (Eds.), *Large Igneous Provinces: continental, oceanic and planetary flood basalts*. Geophysical Monographs Series, vol. 100. American Geophysical Union, pp. 411–438.
- Hoernle, K., 1998. Geochemistry of Jurassic oceanic crust beneath Gran Canaria (Canary Islands): implications for crustal recycling and assimilation. *Journal of Petrology* 39 (5), 859–880.
- Hort, M., 1998. Abrupt change in magma liquidus temperature because of volatile loss or magma mixing: effects on nucleation, crystal growth and thermal history of the magma. *Journal of Petrology* 39, 1063–1076.
- Ionov, D., 2002. Mantle structure and rifting processes in the Baikal–Mongolia region: geophysical data and evidence from xenoliths in volcanic rocks. *Tectonophysics* 351, 41–60.
- Keppie, J.D., 1989. Northern Appalachian terranes and their accretionary history. In: Dallmeyer, R.D. (Ed.), *Terranes in the Circum-Atlantic Paleozoic orogens*. Geological Society of America Special Paper, vol. 230, pp. 159–192.
- Klitgord, K.D., Schouten, H., 1986. Plate Kinematics of the Central Atlantic. In: Vogt, P.R., Tucholke, B.E. (Eds.), *The Geology of North America, Bulletin of Geological Society of America. The Western North Atlantic region (M)*, Boulder, Colorado, pp. 351–378.
- Knight, K.B., Nomade, S., Renne, P.R., Marzoli, A., Bertrand, H., Youbi, N., 2004. The Central Atlantic Magmatic Province at the Triassic–Jurassic boundary: paleomagnetic and  $40\text{Ar}/39\text{Ar}$  evidence from Morocco for brief, episodic volcanism. *Earth and Planetary Science Letters* 228 (1–2), 143–160.
- Kusznir, N.J., Park, R.G., 1987. The extensional strength of the continental lithosphere: its dependence on geothermal gradient, and crustal composition and thickness. In: Coward, M.P., Dewey, J.F., Hancock, P.L. (Eds.), *Continental extensional tectonics*. Geological Society Special Publication, vol. 28, pp. 35–62.
- Langmuir, C.H., Vocke, R.D., Hanson, G.N., 1978. A general mixing equation with applications to Icelandic basalts. *Earth and Planetary Science Letters* 37, 380–392.
- Lassiter, J.C., DePaolo, D.J., 1997. Plume/Lithosphere interaction in the generation of continental and oceanic flood basalts: chemical and isotopic constraints. In: Mahoney, J.J., Coffin, M.F. (Eds.), *Large Igneous Provinces: continental, oceanic and planetary flood basalts*. Geophysical Monographs Series, vol. 100. American Geophysical Union, pp. 335–380.
- Le Bas, M.J., Le Maitre, R.W., Streckeisen, A., Zanetti, B., 1986. A chemical classification of volcanic rocks based on the total alkalis–silica diagram. *Journal of Petrology* 27 (3), 745–750.
- Lowenstern, J.B., 2000. A review of the contrasting behaviour of two magmatic volatiles: chlorine and carbon dioxide. *Journal of Geochemical Exploration* 69–70, 287–290.
- MacDonald, G.A., Katsura, T., 1964. Chemical composition of Hawaiian lavas. *Journal of Petrology* 5, 83–133.
- Manuppella, G., 1988. *Litostratigrafia e Tectónica da Bacia Algarvia*. Geonovas (Lisboa) 10, 67–71.

- Manuppella, G., 1992. Carta Geológica da Região do Algarve. Serviços Geológicos de Portugal; 2 sheets at the 1:100.000 scale and Explanatory Note.
- Martins, L.T., 1991. *Actividade Ígnea Mesozóica em Portugal (Contribuição Petroológica e Geoquímica)*. PhD thesis, University of Lisbon, Portugal, 418 pp.
- Martins, L.T., Kerrich, R., 1998. Magmatismo toleítico continental no Algarve (Sul de Portugal): Um exemplo de contaminação crustal “in situ”. *Comunicações do Instituto Geológico e Mineiro* 85, 99–116.
- Marzoli, A., Renne, P.E., Piccirillo, E.M., Ernesto, M., Bellieni, G., De Min, A., 1999. Extensive 200-million-year-old continental flood basalts of Central Atlantic Magmatic Province. *Science* 284, 616–618.
- Marzoli, A., Bertrand, H., Knight, K.B., Cirilli, S., Buratti, N., Verati, C., Nomade, S., Renne, P.R., Youbi, N., Martini, R., Allenbach, K., Neuwerth, R., Rapaille, C., Zaninetti, L., Bellieni, G., 2004. Synchrony of the Central Atlantic magmatic province and the Triassic–Jurassic boundary climatic and biotic crisis. *Geology* 32, 973–976.
- Mata, J., Kerrich, R., Mac Rae, N.D., Wu, T.-W., 1998. Elemental and isotopic (Sr, Nd, and Pb) characteristics of Madeira Island basalts: evidence for a composite HIMU-EM I plume fertilizing lithosphere. *Canadian Journal of Earth Sciences* 35, 980–997.
- Mata, J., Martins, L.T., Terrinha, P., Munhá, J., Madeira, J., Youbi, N., Miranda, L., 2006. Phanerozoic rifting events on the western Iberia Peninsula: rifting mechanisms and the legacy of previous structures. VII Congresso Nacional de Geologia (Estremoz) 39–42 (Sociedade Geológica de Portugal).
- McArthur, J.M., Howarth, R.J., Bailey, T.R., 2001. Strontium isotope stratigraphy: LOWESS Version 3: best fit to the marine Sr-isotope Curve for 0–509Ma and accompanying look-up table for deriving numerical age. *Journal of Geology* 109, 155–170.
- McHone, J.G., 2000. Non-plume magmatism and rifting during the opening of the central Atlantic Ocean. *Tectonophysics* 316, 287–296.
- McHone, J.G., Puffer, J.H., 2003. Flood basalt province of the Pangean Atlantic rift: regional extent and environmental significance. In: LeTourneau, P.M., Olsen, P.E. (Eds.), *The great rift valleys of Pangea in Eastern North America, Aspects of Triassic–Jurassic Rift Basin Geoscience*, vol. 1. Columbia University Press, pp. 141–154.
- Medina, F., 1995. Syn- and postrift evolution of the El Jadida-Agadir basin (Morocco): constraints for the rifting models of the Central Atlantic. *Canadian Journal of Earth Sciences* 32, 1273–1291.
- Medina, F., 2000. Structural styles of the Moroccan Triassic basins. *Zentralblatt für Geologie und Paläontologie, Teil 1* 9–10, 1167–1192 (Epicontinental Triassic International Symposium).
- Munhá, J.M., 1981. *Igneous and metamorphic petrology of the Iberian Pyrite Belt*. PhD thesis, University of Western Ontario, Canada, 2 vol., 711 p.
- Nomade, S., Poulet, A., Chen, Y., 2002. The French Guyana doleritic dykes: geochemical evidence of three populations and new data for the Jurassic Central Atlantic Magmatic Province. *Journal of Geodynamics* 34, 595–614.
- Nomade, S., Knight, K.B., Beutel, E., Renne, P.R., Verati, C., Féraud, G., Marzoli, A., Youbi, N., Bertrand, N., 2007. Chronology of the Central Atlantic Magmatic Province: Implications for the Central Atlantic rifting processes and the Triassic–Jurassic biotic crisis. *Palaeogeography, Palaeoclimatology, Palaeoecology* 224, 326–344.
- Olsen, P.E., 1999. Giant lava flows, mass extinctions and mantle plumes. *Science* 284, 604–605.
- Oyarzun, R., Doblas, M., López-Ruiz, J., Cebriá, J.M., 1997. Opening of the central Atlantic and asymmetric mantle upwelling phenomena: implications for long-lived magmatism in western North Africa and Europe. *Geology* 25, 727–730.
- Palencia Ortas, A., Osete, M.L., Vegas, R., Silva, P., 2006. Paleomagnetic study of the Messejana Plasencia dyke (Portugal and Spain): a lower Jurassic paleopole for the Iberian plate. *Tectonophysics* 420 (3–4), 455–472.
- Putirka, K., Mikaelian, H., Ryerson, F.J., Shaw, H., 2003. New clinopyroxene-liquid thermobarometers for mafic, evolved and volatile-bearing lava compositions, with applications to lavas from Tibet and the Snake River Plain. *American Mineralogist* 88, 1542–1554.
- Palain, C., 1979. Connaissances stratigraphiques sur la base du mésozoïque portugais. *Ciências da Terra* 5 (Universidade Nova de Lisboa), 11–28.
- Palme, H., O’Neill, H., 2003. Cosmochemical estimates of mantle compositions. In: Carlson, R. (Ed.), *The Mantle and Core. Treatise on Geochemistry*, vol. 2. Elsevier, Washington, pp. 1–38.
- Papike, J.J., Cameron, K.L., Baldwin, K., 1974. Amphiboles and pyroxenes: characterization of other than quadrilateral components and estimates of ferric iron microprobe data. *Geologic Society of America. Abstracts with Programs* 6 (7), 1053–1054.
- Rainbird, R.H., Ernst, R.E., 2001. The sedimentary record of mantle plume uplift. In: Ernst, R.E., Buchan, K.L. (Eds.), *Mantle Plumes: Their identification Through Time*. Geological Society of America Special Paper, vol. 352, pp. 227–245.
- Rey, J., 1983. Le Crétacé de l’Algarve: essai de synthèse. *Comunicações dos Serviços Geológicos de Portugal* 69, 87–101.
- Rocha, R.B., 1976. *Estudo estratigráfico e paleontológico do Jurássico do Algarve Ocidental*. Ciências da Terra 2, 1–178 (Universidade Nova de Lisboa).
- Rudnick, R.L., Gao, S., 2003. The composition of the continental crust. In: Rudnick, R.L. (Ed.), *The Crust*, vol. 3 of Holland, H.D. and Turekian, K.K. (Eds.), *Treatise on Geochemistry*, Elsevier-Pergamon, Oxford, 1–64.
- Ruellan, E., 1985. *Géologie des marges continentales passives: évolution de la marge atlantique du Maroc (Mazagan); étude par submersible seabeam et sismique réflexion. Comparaison avec la marge NW africaine et la marge homologue E américaine*. PhD thesis, Université de Bretagne Occidentale, Brest, 297 p.
- Ruellan, E., Auzende, J.M., Dostmann, H., 1985. Structure and evolution of the Mazagan (El Jadida) plateau and escarpment off central Morocco. *Oceanologica Acta* 5, 59–72.
- Ruppel, C., 1995. Extensional processes in continental lithosphere. *Journal of Geophysical Research* 100, 24187–24215.
- Sahabi, M., Aslanian, D., Olivet, J.L., 2004. Un nouveau point de départ pour l’histoire de l’Atlantique central. *Comptes Rendus de l’Académie des Sciences de Paris* 336, 1041–1052.
- Schermerhorn, L.J., Priem, H.N., Boelrijk, N.A., Hebeda, E.H., Verdurmen, E.A., Verschure, R.H., 1978. Age and origin of the Messejana dolerite fault-dike system (Portugal and Spain) in the light of the opening of the North Atlantic Ocean. *Journal of Geology* 86, 299–309.
- Schlanger, S.O., 1985. Strontium storage and release during deposition and diagenesis of marine carbonates in relation to sea-level variations. In: Lerman, A., Meybeck, M. (Eds.), *Physical and Chemical Weathering in Geochemical Cycles*. NATO ASI Series C, vol. 251, pp. 323–339.
- Schmincke, H.-U., Klügel, A., Hansteen, T.H., Hoernle, K., Bogaard, P.A., 1998. Samples from the Jurassic ocean crust beneath Gran Canaria, La Palma and Lazarote (Canary Islands). *Earth and Planetary Science Letters* 163, 343–360.
- Schott, J.J., Montigny, R., Thuizat, R., 1981. Paleomagnetism and potassium–argon age of the Messejana dyke (Portugal and Spain): angular limitation to the rotation of the Iberian Peninsula since the middle Jurassic. *Earth and Planetary Science Letters* 53, 457–470.

- Sebai, A., Féraud, G., Bertrand, H., Hanes, J., 1991.  $^{40}\text{Ar}/^{39}\text{Ar}$  dating and geochemistry of tholeiitic magmatism related to the early opening of the Central Atlantic rift. *Earth and Planetary Science Letters* 104, 455–472.
- Sears, J.W., St. George, G.M., Winne, J.C., 2005. Continental rift systems and anorogenic magmatism. *Lithos* 80 (1–4), 147–154.
- Sengor, A.M.C., Burke, K., 1978. Relative timing of rifting and volcanism of Earth and its tectonic implications. *Geophysical Research Letters* 5, 419–421.
- Sheth, H.C., 1999. A historical approach to continental flood basalt volcanism: insights into pre-volcanic rifting, sedimentation, and early alkaline magmatism. *Earth and Planetary Science Letters* 168, 19–26.
- Skilling, I.P., White, J.D.L., McPhie, J., 2002. Peperite: a review of magma-sediment mingling. *Journal of Volcanology and Geothermal Research* 114, 1–17.
- Stapel, G., Cloetingh, S., Pronk, B., 1996. Quantitative subsidence analysis of the Mesozoic evolution of the Lusitanian basin (western Iberian margin). *Tectonophysics* 266, 493–507.
- Sun, S.-S., McDonough, W.F., 1989. Chemical and isotopic systematics of oceanic basalts: implication for mantle composition and processes. In: Saunders, A.D., Norry, M. (Eds.), *Magmatism in the Ocean Basins*. *Journal of the Geological Society of London*, vol. 42, pp. 313–345.
- Terrinha, P., Ribeiro, C., Kullberg, J.C., Lopes, C., Rocha, R., Ribeiro, A., 2002. Compressive episodes and faunal isolation during rifting, Southwest Iberia. *The Journal of Geology* 110, 101–113.
- Tommasi, A., Vauchez, A., 2001. Continental rifting parallel to ancient collisional belts: an effect of the mechanical anisotropy of the lithospheric mantle. *Earth and Planetary Science Letters* 185, 199–210.
- Turcotte, D.L., Emerman, S.H., 1983. Mechanisms of active and passive rifting. *Tectonophysics* 94, 39–50.
- Valley, J.W., 1986. Stable isotope geochemistry of metamorphic rocks. In: Valley, J.W., Taylor, H.P., O'Neil, J.R. (Eds.), *Stable Isotopes in High Temperature Geological Processes*. *Reviews in Mineralogy*, 16, pp. 445–490.
- Veizer, J., 2004. Isotope Data, Phanerozoic database,  $\delta^{18}\text{O}$  update-2004: [http://www.science.uottawa.ca/geology/isotope\\_data/](http://www.science.uottawa.ca/geology/isotope_data/).
- Veizer, J., Ala, D., Azmy, K., Bruckschen, P., Buhl, D., Bruhn, F., Carden, G.A.F., Diener, A., Ebner, S., Godderis, Y., Jasper, T., Korte, C., Pawellek, F., Podlaha, O.G., Strauss, H., 1999.  $^{87}\text{Sr}/^{86}\text{Sr}$ ,  $\delta^{13}\text{C}$  and  $\delta^{18}\text{O}$  evolution of Phanerozoic seawater. *Chemical Geology* 161, 59–88.
- Verati, C., Bertrand, H., Féraud, G., 2005. The farthest record of the Central Atlantic Magmatic Province into West Africa craton: Precise  $^{40}\text{Ar}/^{39}\text{Ar}$  dating and geochemistry of Taodenni basin intrusives (northern Mali). *Earth and Planetary Science Letters* 235, 391–407.
- Verati, C., Rapaille, C., Féraud, G., Marzoli, A., Bertrand, H., Youbi, N., 2007.  $^{40}\text{Ar}/^{39}\text{Ar}$  ages and duration of the Central Atlantic Magmatic Province volcanism in Morocco and Portugal and its relation to the Triassic–Jurassic boundary. *Palaeogeography, Palaeoclimatology, Palaeoecology*. doi:10.1016/j.palaeo.2006.06.033.
- Vollmer, R., 1976. Rb–Sr and U–Th–Pb systematics of alkaline rocks: the alkaline rocks from Italy. *Geochimica et Cosmochimica Acta* 40, 283–295.
- Westrich, H.R., Stockman, H.W., Eichelberger, J.C., 1988. Degassing of rhyolite magma during ascent and emplacement. *Journal of Geophysical Research* 93, 6503–6511.
- White, J.D.L., Houghton, B.F., 2006. Primary volcanoclastic rocks. *Geology* 34 (8), 677–680.
- Wilson, M., 1997. Thermal evolution of the Central Atlantic passive margins: continental break-up above a Mesozoic superplume. *Journal of the Geological Society of London* 154, 491–495.
- Wilson, M., Downes, H., 1991. Tertiary–Quaternary extension-related alkaline magmatism in Western and Central Europe. *Journal of Petrology* 32, 811–849.
- Withjack, M.O., Schlische, R.W., Olsen, P.E., 1998. Diachronous rifting, drifting, and inversion on the passive margin of central eastern north america: an analog for other passive margins. *Association of the American Petroleum Geologists Bulletin* 82 (5A), 817–835.
- Youbi, N., Martins, L., Munhá, J., Ibouh, H., Madeira, J., Aït Chayeb, E.H., El Boukhari, A., 2003. The Late Triassic–Early Jurassic Volcanism of Morocco and Portugal in the framework of the Central Atlantic Magmatic Province. In: Hames, W.E., McHone, J.G., Renne, P.R., Ruppel, C. (Eds.), *The Central Atlantic Magmatic Province: Insights From Fragments of Pangea*. *Geophysical Monographs Series American Geophysical Union*, vol. 136, pp. 179–207. doi:10.1029/136GM10.